Norwegian University
of Life Sciences

Master's Thesis 2021 60 ECTS
Faculty of Chemistry, Biotechnology and Food Science

Effect of calcium on fatty acid digestibility and weight development in mice

Sebastian Meling
Biotechnology – Molecular Biology

Effect of calcium on fatty acid digestibility and weight development in mice

Sebastian Meling

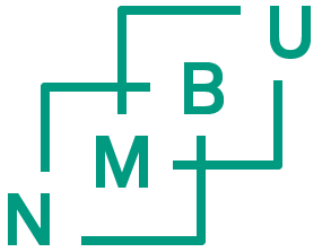

Supervisors:

Harald Carlsen
Siv Borghild Skeie
Gyrd Omholt Gjevestad

Master thesis

Faculty of Chemistry, Biotechnology and Food science

Norwegian University of Life Sciences

August 2021

Effect of calcium on fatty acid digestibility and weight development in mice

https://nmbu.brage.unit.no

ACKNOWLEDGEMENTS

This master thesis was conducted as part of a two-year master program in Biotechnology at the Department of Chemistry, Biotechnology and Food Science (KBM) at the Norwegian University of Life Science (NMBU) from August 2020 to August 2021.

First and foremost, I would like to thank my main supervisor, professor Harald Carlsen for your guidance and support throughout the year. You have been a true inspiration, and I have learnt much from you. I have cherished our conversations, whether about cheese, mice, TV series or music.

Furthermore, I would like to thank my co-supervisors, PhD Gyrd Omholdt Gjevestad and professor Siv Skeie, for their valuable input. I would also like to thank PhD-student Dimitrios Papoutsis, who has been a mentor from the start and never hesitate to offer help. You spent many hours in the animal lab with us and countless hours analysing my samples during the lockdown. I am deeply grateful.

Moreover, I would like to express my gratitude to Senior Engineer Hanne Devle, who guided us expertly into the world of analytical chemistry.

Thank you to associate professor Siv Kjølsrud Bøhn who helped me in my most stressful hours. You are incredibly kind.

I am grateful for the friendships of master student Marte Uglum and PhD-student Anne Mari Herfindal. You were always there during the digital lunch meeting, which I am convinced was essential to completing this master thesis. Marte, you have been a fantastic partner throughout the year; I could not have done this without you.

Finally, I would like to thank my girlfriend and my parents for their endless support throughout this year.

ABSTRACT

Background: High intake of saturated fatty acids (SFA) has consistently been shown to raise low-density lipoprotein cholesterol, a known risk factor of cardiovascular disease (CVD). One of the most significant contributors of SFAs to the adult diet is cheese. While containing high amounts of SFAs, cheese itself does not seem to increase the risk of disease. The high calcium (Ca) content in cheese has been proposed to explain this paradox through limiting the uptake of long-chain SFAs by forming insoluble soaps. Also, other abilities of the cheese have been suggested to affect SFA uptake through a so-called matrix effect.

Aim: We aimed to determine whether fatty acid (FA) digestibility, weight development and changes in body fat mass was affected by Ca and type of matrix (cheese versus butter) in mice. Furthermore, we wanted to investigate whether Ca and differences in food matrix affected intestinal health. Finally, we wanted to assess the accuracy of a nuclear magnetic resonance (NMR) instrument from Bruker on determining body fat in live mice.

Methods: Male mice (C57BL/6JRj) were fed a high-fat (HF) diet with FAs either from cheese (n=20) or butter (n=30) and received varying Ca levels [low-Ca (2g/kg feed), medium-Ca (7g/kg feed) and high-Ca (20g/kg feed)] for 5 weeks. A control group received a low-fat chow diet with a standard Ca content of 5g/kg (n=10). Food consumption and weight were registered weekly. Furthermore, fat mass was measured weekly using a body composition analyser (Minispec LF50, Bruker) and faeces were collected every day during week 4. A method was developed to quantify the FA content in faeces and food which was used to calculate % digestibility = (FA consumed – FA excreted) * $(\text{FA consumed})^{-1}$ x 100. Upon termination of the animals, the mucosal tissues were harvested from the small intestines, and the expression of genes related to inflammation and intestinal barrier function were analysed using real-time polymerase chain reaction (RT-PCR). NMR fat mass measurements were compared to the weight of dissected large fat depots in the same mice to evaluate the accuracy of the instrument.

Results: Our results show that Ca impacts FA digestibility in mice receiving HF diets, in a dose dependent manner. Mice on a high-Ca/HF diet had 2.5% lower uptake of Palmitic acid (16:0) and 6% lower uptake of Stearic acid (18:0) compared to mice fed a low-Ca/HF-based diet. Ca content also affected weight gain in the mice that received HF butter-based diets with a lower weight gain (-9%) in the high-Ca group compared to the low-Ca group. No effects of Ca were found on fat mass development. Furthermore, no matrix effect was observed on 16:0 and 18:0 digestibility, but there was a trend that the matrix affected weight development of the mice. Overall, no effects of Ca were seen on the expression of inflammation markers in the small intestine. However, the tight junction gene ZO-1 had the highest expression in HF fed mice with low Ca levels (butter-based HF diet) and medium Ca levels (cheese-based HF diet). In addition, the matrix was found to significantly influence the expression of *ZO-1*, with a higher expression being observed in the cheese-based diets. Finally, the NMR instrument emerged as a reliable and good predictor of body fat mass in mice.

Conclusion: We found Ca to impact SFA digestibility, but to a lesser extent than shown in the literature. The reduction in FA digestibility cannot explain the difference in weight gain between the groups, which might be due different metabolic activity in the mice or an effect of the matrix. Expression of the tight junction gene *ZO-1* was found to be influenced by Ca and matrix. Further research is needed to elucidate the interplay between Ca and fat, and how this affects disease development.

Content

FIGURES

TABLES

ABBREVIATIONS

ACS1	Acyl-CoA synthetase 1
ANOVA	Analysis of variance
Ca	Calcium
CCK	Cholecystokinin
cDNA	Complementary DNA
CM	Chylomicron
CS	Calcium soaps
Ct	Cycle threshold
CVD	Cardiovascular disease
DAG	Diacylglycerol
DHA	Docosahexaenoic
DNA	Deoxyribonucleic acid
dNTP	Deoxyribonucleotide triphosphate
dsDNA	Double-stranded DNA
EDTA	Ethylenediaminetetraacetic acid
EPA	Eicosapentaenoic
FA	Fatty acid
FABPc	Cytoplasmic FABP
FAME	Fatty acid methyl esters
FATP4	Fatty acid transport protein 4
FFA	Free fatty acid
FID	Flame ionisation detector
GAPDH	Glyceraldehyde 3-phosphate dehydrogenase
GC	Gas chromatography
GC-MS	Gas chromatography–mass spectrometry
GI	Gastrointestinal
HF	High-fat
HKG	Housekeeping gene
IL	Interleukin
iNOS	Nitric oxide synthase
IS	Internal standard
IUPAC	International union of pure and applied chemistry

K	Potassium
LDL	Low-density lipoprotein
LPS	Lipopolysaccharide
MAG	Monoacylglycerol
MDB	Membrane desalting buffer
MESA	Multi-Ethnic Study of Atherosclerosis
Mg	Magnesium
MMLV	Moloney murine leukaemia virus
mRNA	Messenger ribonucleic acid
MTTP	Microsomal triglyceride transfer protein
MUFA	Monosaturated fatty acid
Na	Sodium
NHS	Nurses' Health Study
NL	Neutral lipid
NMBU	Norwegian University of Life Science
NMR	Nuclear magnetic resonance
NOX2	NADPH oxidase 2
NTNU	Norwegian University of Science and Technology
P	Phosphorus
PAMP	Pathogen-associated molecular pattern
PBS	Phosphate-buffered saline
PCR	Polymerase chain reaction
PPAR	Peroxisome proliferator-activated receptor
PRR	Pattern recognizing receptors
PUFA	Polysaturated fatty acid
RIN	RNA integrity number
RNS	Reactive nitrogen species
ROS	Reactive oxygen species
RT	Reverse transcriptase
RT-PCR	Real-time polymerase chain reaction
S	Sulphur
SFA	Saturated fatty acid
SPE	Solid-phase extraction
ssDNA	Single-stranded DNA

TAG	Triacylglycerol
TD-NMR	Time-domain nuclear magnetic resonance
TLR4	Toll-like receptor 4
TNF-α	Tumor necrosis factor α
TNO	Netherlands Organisation for Applied Scientific Research
UiO	University of Oslo
ZO	Zonula occludens
β-ME	β-mercaptoethanol

1 INTRODUCTION

1.1 Lipids and dietary fats

Lipids are a diverse gathering of organic compounds involved in many mechanisms in the human body. The defining feature of a lipid is that it will be soluble in a non-polar solvent. More commonly, we think of lipids as molecules that are not easily dissolved in water, such as triacylglycerols (TAGs), most free fatty acids (FFAs) and cholesterol esters; they are hydrophobic compounds (water-fearing). However, not all lipids are entirely hydrophobic, as some will exhibit both hydrophilic (water-loving) and hydrophobic traits. Such compounds are classified as amphiphilic or amphipathic. An example is phospholipids, an integral part of the membranes of cells and organelles.

The word "lipid" is not commonly used among the general population; the term "fat" is far more prevalent. Dietary fats are lipids ingested through the diet. The most abundant form of dietary fat is TAG, which constitutes 90-95% of the fat from the diet (Iqbal & Hussain, 2009). The remaining percentages are phospholipids, sterols (e.g., cholesterol) and some fat-soluble vitamins (i.e., vitamins A, D, E and K) (Iqbal & Hussain, 2009). Fat is the most energy-dense of the macronutrients, supplying 9 kcal/g, whereas carbohydrates and proteins supply 4 kcal/g (Wang et al., 2013). In Norway, dietary fat provides approximately 30-40% of the energy from food among adults, presented in the NORKOST 3 study, (Totland et al., 2012) which falls within the recommended fat intake of the country's dietary guidelines (25-40E%). The dietary guidelines are even more specific: they recommend monounsaturated fatty acids (FAs) to account for 10-20 % of the energy from the diet, polyunsaturated FAs to account for 5-10% and saturated fatty acids (SFAs) to account for less than 10 energy percent (Nordic Nutrition Recommendations 2012). The NORKOST 3 study revealed that the energy intake from mono- and polyunsaturated FAs fell within the recommended ranges at 12E% and 6.2E%, respectively. However, saturated fats accounted for 13% of the energy in the diet, which is more than what the government recommends. The most common sources of dietary fats in the Norwegian diet are that of butter and oils (23% of total fat intake), meat and meat products (20% of total fat intake), and cheese (12% of total fat intake) (Totland et al., 2012).

Fat serves a multitude of essential functions in the body. First and foremost, fat serves as energy storage. Adipose (fat) cells store fat, and thus also energy, in the form of TAG molecules. Utilisation of energy from adipose tissue can only occur when insulin levels are low, a state observed during fasting and exercise. Lipases will cleave the ester bonds between the FAs and the glycerol, thus releasing energy to be used where needed (Cohen & Spiegelman, 2016). Second, fat is an integral part of the cell membranes. The attributes of amphipathic lipids spontaneously drive the cellular membrane formation; the hydrophobic parts will seek together in an aqueous environment, while the hydrophilic parts will interact with the surrounding water (van Meer et al., 2008). The cell membrane of animal cells is also rich in cholesterol,

which makes up about 30% of the lipid bilayer (Zhang et al., 2019). Third, fat can provide molecules used in signalling. An example is Arachidonic acid which is a precursor for many signalling lipids. It is a polyunsaturated FA connected to phospholipids in the cell membrane. If specific receptors are activated, the FA can be released from the membrane, which will trigger a cascade of events that ultimately leads to the creation of signalling lipids (Dhall et al., 2015). Finally, some FAs regulate gene expression by acting as a ligand to the peroxisome proliferator-activated receptors (PPARs). The PPARs are part of a subfamily of nuclear receptors that are crucial regulators in lipid metabolism and inflammation. They form heterodimers with another subfamily of nuclear receptors, retinoid X receptors, and can subsequently bind to specific deoxyribonucleic acid (DNA) sequences, thus regulating gene expression (Varga et al., 2011).

1.2 Dietary fats; structure and nomenclature

The most abundant form of dietary fat is TAG, which constitutes 90-95% of the fat from the diet (Iqbal & Hussain, 2009). The backbone of the TAG molecule is a 3-carbon glycerol. The glycerol-carbons are numbered stereo-specifically as *sn1*, *sn2* and *sn3*. To each of the carbons, a FA is connected by an ester binding. A FA is made up of an aliphatic carbon chain with a carboxylic acid functional group at the end. The carbon chain length will often be used to classify the FA: short-chain FAs have a chain of 2-6 carbons, medium-chain FAs have a chain of 6-12 carbons, long-chain FAs have a chain of 13-21 carbons, while very-long-chain FAs have 22 carbons or more.

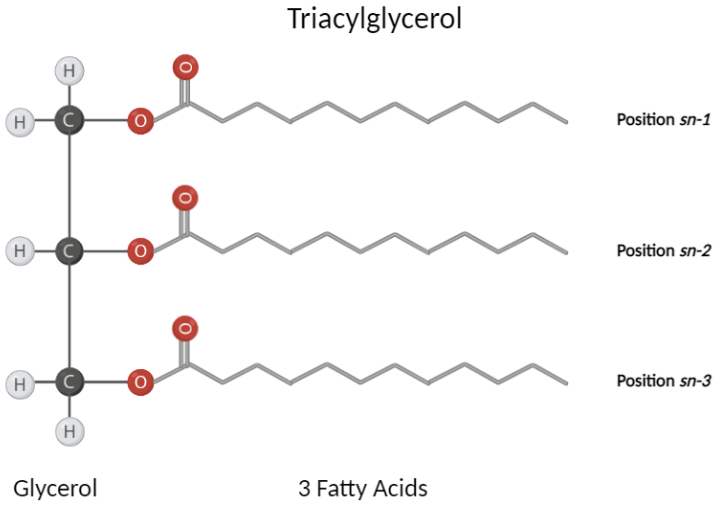

Figure 1.1: General structure of a triacylglycerol. The figure visualises a general structure of a TAG molecule. The backbone consists of a glycerol molecule of 3 carbons, connected to three FAs by ester bindings. The three carbons in the glycerol molecule represents positions, namely *sn1*, *sn2*, and *sn3*. The structure in the figure is simplified, as the molecule often consists of FAs with different chain lengths, where the shortest usually is placed at the *sn1*-position. The figure is created using BioRender,com. Abbreviations: TAG = Triacylglycerol, FA = Fatty acid

SFAs only have single bonds between the atoms of the hydrocarbon chain. The carbon atoms in the chain all bind to four other atoms, resulting in a complete degree of saturation. An introduction of one double bond to the hydrocarbon chain creates a monounsaturated fatty acid (MUFA). Furthermore, FAs with more than one double bond are categorised as polyunsaturated fatty acids (PUFAs). Double bonds alter the physical and chemical properties of the FAs, as they often lead to a branching of the hydrocarbon chain, in contrast to a SFAs whose hydrocarbon chain will be straight. The branching of the chain affects the fluidity of cell membranes. Due to their straight hydrocarbon chain, SFA can be more tightly packed, resulting in a less fluid membrane. Unsaturated FAs result in a more fluid membrane due to their less structured packing (Ballweg et al., 2020).

There are several ways of naming FAs. The FAs have a common name, usually derived from where the FA was first discovered (i.e., palmitic acid was discovered in palm oil). Additionally, FAs are given an international union of pure and applied chemistry (IUPAC) name that chemists typically prefer. However, nutritionists prefer the omega nomenclature method to name FAs. The method is based on how many carbon atoms the hydrocarbon chain is composed of. The amount of double bonds in the hydrocarbon chain is also specified. Finally, the first double bond placement is given by counting carbons from the methyl end of the FA (e.g., 18:1ω-6). An overview of standard FAs with their common- and omega name is given in (Table 1.1).

Table 1.1: Nomenclature of fatty acids commonly found in food

	Common Name	**Omega Name**	**IUPAC Name**
Saturated Fatty Acids	Capric	10:0	Decanoic
	Lauric	12:0	Dodecanoic
	Myristic	14:0	Tetradecanoic
	Palmatic	16:0	Hexadecanoic
	Stearic	18:0	Octadecanoic
	Arachidic	20:0	Icosanoic
Monounsaturated Fatty Acids	Caproleic	10:1	Dec-9-enoic
	Lauroleic	12:1ω-3	(Z)-dodec-9-enoic
	Myristoleic	14:1ω-5	(Z)-tetradec-9-enoic
	Palmitoleic	16:1ω-7	(Z)-hexadec-9-enoic
	Oleic	18:1ω-9	(Z)-octadec-9-enoic
	Gadoleic	20:1ω-11	(Z)-icos-9-enoic
Polyunsaturated Fatty Acids	Linoleic	18:2ω-6	(9Z,12Z)-octadeca-9,12-dienoic
	Alpha-linoleic	18:3ω-3	(9Z,12Z,15Z)-octadeca-9,12,15-trienoic
	Arachidonic	20:4ω-6	(5Z,8Z,11Z,14Z)-icosa-5,8,11,14-tetraenoic
	Eicosapentaenoic (EPA)	20:5ω-3	(5Z,8Z,11Z,14Z,17Z)-icosa-5,8,11,14,17-pentaenoic
	Docosahexaenoic (DHA)	22:6ω-3	(4Z,7Z,10Z,13Z,16Z,19Z)-docosa-4,7,10,13,16,19-hexaenoic

Abbreviations: IUPAC = International union of pure and applied chemistry

1.3 Fat digestion and absorption

One could argue that the digestion process starts at first sight and smell, or even thought, of food. Pavlov famously demonstrated this when he managed to induce salivation in dogs by the sounds of a bell, a sound the dogs had been trained to associate with feeding (Rehman et al., 2021). Indeed, a number of physiological processes are induced along the digestive tract by this first phase of digestion. The act of chewing breaks down the food into smaller pieces, which are more easily digested. Chewing induces the release of saliva to the mouth cavity, which moistens the food and aids in creating a food bolus to be more easily swallowed. While saliva is 98% water, it also contains digestive enzymes like amylase and lingual lipase (Pedersen et al., 2002).

Digestion of TAG is made possible by three lipases; lingual lipase, gastric lipase and pancreatic lipase. They all hydrolyse the ester binding between the glycerol backbone and the carboxyl part of the fatty acid. However, the lipases work in different locations and have somewhat different outcomes. When the food enters the mouth cavity, the lingual lipase is secreted from the "von Ebner" glands (Kulkarni & Mattes, 2014). Lingual lipase can penetrate milk fat globules, making it a key player in infant digestion of fat. However, in adults, lingual lipase is less important. Evidence suggests that lingual lipase will be moderately active in the mouth cavity; however, it will travel with the food bolus to the stomach and continue its lipolytic activity there (Kulkarni & Mattes, 2014). In the stomach, gastric lipase is secreted from chief cells in the gastric mucosa (Tomasik et al., 2013). The preduodenal lipases (i.e., lingual and gastric lipase) both hydrolyse the ester bond in the *sn-3* position of the TAG molecule, leaving the end products of diacylglycerol (DAG) and one FFA (Mu & Høy, 2004). The preduodenal lipases are accountable for about 30% of TAG hydrolysis. However, most TAG molecules (70%) escape preduodenal digestion and reach the small intestine intact to be broken down by pancreatic lipase in the duodenum (Kulkarni & Mattes, 2014).

Dietary fats all share hydrophobic traits, causing them to clump together into large fat droplets when presented to the aqueous environment of the gastrointestinal (GI) tract. The fat droplet is subsequently coated with bile acids and phospholipids, as seen in figure 1.2. These are amphiphilic molecules showing both lipophilic and hydrophilic traits. Hence, the dietary lipids work in unison with other available molecules to create an emulsified lipid droplet. The emulsification consists of hydrophobic (lipophilic) compounds on the inside, like TAG and cholesterol esters. Essential for this process are amphiphilic compounds like phospholipids, bile salts and FAs which will turn their lipophilic part towards the inside of the fat droplet. Most of these amphiphilic molecules are commonly called bile stored in the gall bladder and released during food ingestion. Meanwhile the hydrophilic part of the lipid droplet will be facing the outside aqueous environment. The introduction of bile will break up the large lipid droplets into smaller droplets. The smaller emulsified lipid droplets will have an increased surface area, making them more accessible to digestive enzymes (Murota, 2020). Many crucial digestive steps take place at the surface of

the lipid droplet where fat meets water. In this master thesis, the term "interface/interfacial" will refer to the site at which water and fat meet in the lipid droplet.

Most of the fat digestion occurs in the duodenum. The presence of lipid digestion products arriving from the stomach will stimulate secretion of the hormone cholecystokinin (CCK) from enteroendocrine cells in the mucosa. CCK is key for stimulating release of digestive juices from both pancreas and gall bladder that will empty into the lumen of the duodenum. i.e., the gall bladder, which contains bile, will contract under the influence of CCK and enzymes and bicarbonate from the pancreas are stimulated. Subsequently, the lipid emulsions will be coated with bile and pancreatic juice. This process significantly changes the structure and chemical properties of the droplet (Wang et al., 2013), and the surface area of the droplet increase, allowing for increased enzymatic activity. Unlike the preduodenal lipases, pancreatic lipase is dependent on co-lipase to function, as the pancreatic lipase cannot bind effectively to the lipid droplets in the absence of co-lipase. With co-lipase present in the lipid-water interface, pancreatic lipase can bind to the droplet and facilitate fat digestion (Huang et al., 2012). The pancreatic lipase hydrolyses the ester bonds in the *sn1* and *sn3*-position of the TAG molecule, resulting in a *sn2*-monoacylglycerol (MAG) and two FFAs. About 25% of the FAs in the *sn2*-MAG molecules will migrate to the *sn1,3*-positions, thus becoming available for hydrolysis by pancreatic lipase and subsequent absorption. The remaining 75% of *sn2*-MAGs will generally be incorporated into mixed micelles and subsequently absorbed by the enterocytes (Mu & Høy, 2004).

Intact fat (mostly TAGs) will be transported from the core of the lipid droplet to the interface, where TAGs are hydrolysed by pancreatic lipase to yield two FFAs and one *sn2*-MAG. Mixed micelles are created as digested lipids bud off from the lipid droplet. They are a mixture of FAs, MAGs, diacylglycerols (DAGs), phospholipids, cholesterol, fat-soluble vitamins and bile acids. The mixed micelles are essential for the uptake of lipids, as they transport the lipids across the unstirred water layer adjacent to the outer membrane of the enterocytes. The fat is absorbed at the brush border membrane of the enterocytes. Water-soluble short-chain FAs can pass through the membrane by passive diffusion. While there might be such a mechanism for the water-insoluble FAs, it is believed that the dominant mechanism is that of protein-mediated transport. There are two essential proteins for FA uptake: CD36 and fatty acid transport protein 4 (FATP4). CD36 works alone or in unison with a fatty acid-binding protein (FABPpm) to actively transport medium to long-chain FAs across the apical membrane of the enterocyte. Once inside the cell, the FAs are bound by cytoplasmic FABP (FABPc) before undergoing further metabolic processing. FATP4 also bind medium to long-chain FAs and transport them across the brush border membrane. On the inside, plasma membrane acyl-CoA synthetase 1 (ACS1) is ready to convert the FAs to acyl-coenzyme A esters before the eventual reconstruction of TAG molecules (Wang et al., 2013).

Some short-chain FAs are absorbed directly from the enterocytes in the small intestine to the mesenteric venous blood and subsequently to the portal vein (Wang et al., 2013). However, the mechanism of fat transport and distribution is generally more complex. Intestinal lipoproteins are synthesized in the enterocytes, and upon secretion to the circulation, can deliver TAG to tissues for oxidation or storage. After uptake of FFAs and MAGs into the enterocytes, they are remade into TAG in the smooth endoplasmic reticulum (Mu & Høy, 2004). During the postprandial state, the chylomicron (CM) is the most abundant lipoprotein. While some TAG molecules are incorporated into CM during the assembly process (Mu & Høy, 2004), intestinal microsomal triglyceride transfer protein (MTTP) will transfer TAG into the final synthesized CM in the smooth endoplasmic reticulum. The final composition of the CM is 85-95% TAG, making them an essential part of the fat distribution (Wang et al., 2013). The CMs are secreted into the intestinal lymph and subsequently enter the blood through the thoracic duct. A majority of the TAGs are removed by lipoprotein lipase present at the surface of capillary endothelial cells in muscle and adipose tissue (Mu & Høy, 2004; Wang et al., 2013).

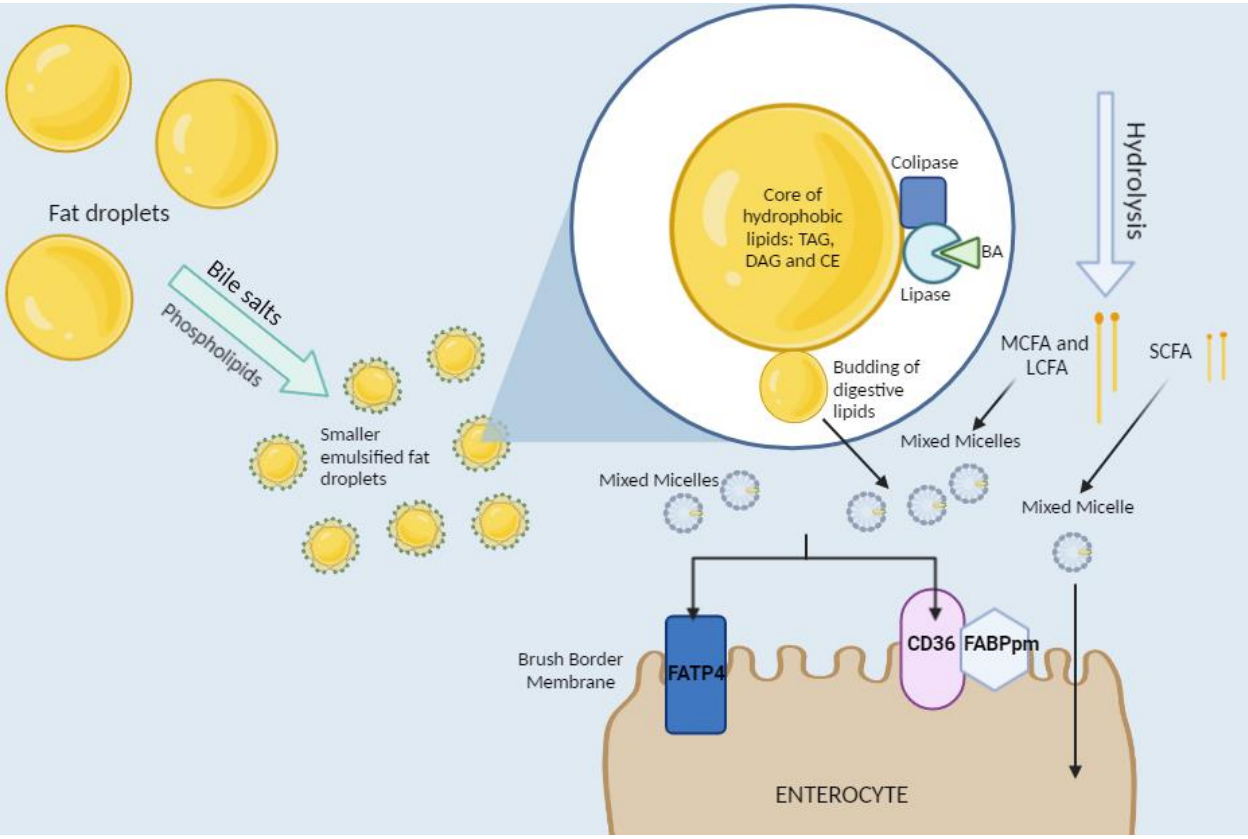

Figure 1.2: An illustration of the fat digestion process. Hydrophobic lipids clump together into large fat droplets in an aqueous environment. The introduction and coating of BA and phospholipids breaks the large droplets into smaller emulsified fat droplets (Murota, 2020). Pancreatic lipase anchors to the interface with the aid of colipase and BA to hydrolyse the TAG in the core of the fat droplet (Huang et al., 2012). Digested lipids buds off the lipid droplet to create mixed micelles, which transports the lipids across the unstirred water layer adjacent to the out membrane of the enterocytes. The proteins CD36 (often aided by FABPpm) and FATP4 facilitate the transport of the FAs from the mixed micelles into the enterocytes (Wang et al., 2013). The figure is created using BioRender,com Abbreviations: TAG = Triacylglycerol, DAG = Diacylglycerol, CE = Cholesterol ester, BA = Bile acids, FABPpm = Fatty acid-binding protein, FATP4 = Fatty acid transport protein 4, FA = Fatty acid, SCFA = Short-chain fatty acid, MCFA = Medium-chain fatty acid, LCFA = Long-chain fatty acid.

1.4 Saturated fats – the villains of dietary fats

A high intake of SFA is associated with high low-density lipoprotein cholesterol levels in the blood, a well-established risk factor for CVD (Lewington et al., 2007). CVD is an umbrella term that includes all diseases affecting the heart or blood vessels (e.g., heart attack, stroke, peripheral artery disease). In line with the diet-heart hypothesis, scientists have for decades suggested that SFAs increase while PUFA decrease the risk of CVD (Dayton et al., 1965; de Lorgeril et al., 1999; Hu et al., 1997; Keys et al., 1986; Kushi et al., 1985). Still, there is discussion in the scientific community about the relationship between total fat and CVD incidence (Howard et al., 2006; Siri-Tarino et al., 2010). In recent years, a more thorough investigation of individual FAs with relation to CVD has been conducted. Carbon chain length may play an essential role in the health implications of SFAs. The Nurses' Health Study (NHS) is a prospective cohort study that, which among other things, studied SFAs with different carbon chain lengths in relation to CVD. They reported that a higher intake of long-chain SFA (12:0, 14:0, 16:0 and 18:0) was associated with elevated risk of CVD, whereas no such associations were found for short- to medium-chain SFAs (4:0-10:0) (Hu et al., 1999).

Additionally, the food source providing the fat might be of importance. Foods have different matrices and compounds which could attenuate or amplify the effects of the fat. For example, processed red meats, a common source of SFA, contain high amounts of sodium which could have inverse effects on CVD (Micha et al., 2010). On the other hand, phytochemicals from plant could potentially decrease the effects of SFA. The Multi-Ethnic Study of Atherosclerosis (MESA) from 2012 investigated how SFAs from different food sources impacted CVD incidence. The study results showed that a high intake of dairy SFAs was associated with a lower risk of CVD, while a high intake of meat SFAs was associated with a higher risk of CVD (de Oliveira Otto et al., 2012). The findings of the NHS and MESA projects underline the need to further research these topics and understand the underlying mechanisms of how SFAs impact human health.

1.5 Cheese

1.5.1 Cheese consumption and composition

Cheese provides a wide range of nutrients to the diet. It is abundant in protein, fat, vitamins and minerals such as Ca, sodium (Na), phosphorus (P), sulphur (S), potassium (K) and magnesium (Mg). The predominant protein of the cheese is casein, as the whey is separated out during the curdling. Moreover, most of the lactose present in milk is separated with the whey, making it a viable option for the lactose-intolerant (Manuelian et al., 2017). Cheese is one of the primary dietary sources of SFA (Huth et al., 2013). SFA makes up approximately 55-73% of bovine milk fat (Mollica et al., 2021; Månsson, 2008), making it a very SFA dense product. Thus, cheese might contribute significantly to the total SFA intake in the population. This statement is strengthened by NORKOST 3, a Norwegian dietary survey of food intake,

which reported that cheese was accountable for 20% of the daily SFA intake in the participants (Totland et al., 2012).

The two most abundant minerals of cheese are Na and Ca. Dairy foods are a notable contributor of Na to the diet as they account for about 11% and 8% of dietary Na in the USA and United Kingdom, respectively. Furthermore, the NORKOST 3 study reported that 7% of the total Na ingested by Norwegian participants was derived from cheese (Totland et al., 2012). Additionally, the abundance of Ca makes cheese (and milk) important in human bone and tooth health. Approximately 60 to 70% of dietary Ca comes from dairy products, with cheese being the most crucial source in adults (Muehlhoff et al., 2013). While Ca is of nutritional benefit to the consumer, the mineral also plays a vital role in the cheese's chemical and physical attributes. Ca has a positive charge and can thus interact with negatively charged casein proteins within the protein matrix of the cheese. Whereas the negatively charged casein proteins are somewhat repelled from each other by having the same charge, the binding of Ca has a neutralising effect, allowing for more tightly packed casein proteins. The effect of Ca on protein interactions are notable in the final product; low Ca cheeses will be softer, melt better and be more stretchy (McMahon et al., 2005).

Dietary guidelines generally recommend about 800-1000mg of Ca daily (Dietary Guidelines for Americans, Nordic Recommendations). Gouda-like cheeses and Cheddar-cheeses typically contain about 700-800 mg Ca per 100 g of cheese (Tunick, 1987). NORKOST 3 reported that participants, on average, ate 44 grams of cheese daily (Totland et al., 2012). However, with pizza contributing to a large proportion of the cheese consumed, it is natural to assume that the daily intake of cheese during a pizza meal is much larger. It is within reason to think that one person could consume 100-200g of cheese when eating pizza. Therefore, during a pizza meal, it would be possible to ingest 1600mg of Ca, approximately doubling the recommended daily requirements in a short time span.

1.5.2 Cheese and health

Cheese and its impact on human health is a heavily debated topic within the field of nutrition. Dairy products have long been a cornerstone of the human diet. Still, overconsumption has become a trademark of the obesity pandemic, prompting a more thorough investigation of potentially harmful products. A defining feature of cheese is its high SFA content. While a high intake of long-chain SFA is associated with a high risk of developing CVD (Hu et al., 1999), a high cheese intake does not seem to increase the risk of CVD (Alexander et al., 2016; O'Sullivan et al., 2013). The O'Sullivan and Alexander articles are both meta-analyses that review the available literature on cheese and CVD risk. While the evidence on cheese consumption and CVD risk is usually neutral to beneficial (de Oliveira Otto et al., 2012), many dietary recommendations still advise to limit the consumption of full-fat dairy products. The lack of a consensus

on the topic makes it difficult for the consumers to make informed decisions as to what dairy products to include in their diet.

While there is some debate about whether cheese in itself is healthy or unhealthy, most agree that despite the high fat content of the product, it does not seem to pose a grave concern to health as one might expect. In particular, when considering the abundance of SFA in cheese, one could expect the association between cheese and disease to be well documented. Nevertheless, this is not the case.

A closer look at the FA composition of the cheese reveals that Palmitic acid (16:0) makes up about 30% of the total fat in the cheese (Månsson, 2008). It is the most abundant SFA in the human body, with 16:0 making up 20-30% of the total FA (Carta et al., 2017). It is a long-chain SFA that consists of a hydrocarbon chain of 16 carbons. 16:0 is often named one of the villains in the world of nutrition, as high consumption will increase the risk of CVD (Harvey et al., 2010; Shen et al., 2013). Additionally, cheese is rich in Stearic acid (18:0) and Myristic acid (14:0), with 18:0 making up about 12% and 14:0 making up about 10% of the total bovine milk fat (Månsson, 2008). 14:0 raises low-density lipoprotein (LDL) cholesterol more than 16:0 and 18:0 (Fattore et al., 2014). A prospective case-control study discovered higher blood levels of 14:0 in patients with CVD than in the control group (Chei et al., 2018). While the literature on 14:0 and 16:0 have negative undertones, the evidence on 18:0 is conflicting. Some report that high consumption of 18:0 will increase CVD risk (Praagman et al., 2019; Zong et al., 2016), while others report no significant associations between the two (Praagman et al., 2016).

1.5.3 Knowledge gaps

Saturated fats have been labelled as "unhealthy fats", and consumers have been warned to limit their intake of SFA for decades. SFA will raise LDL cholesterol which is a known risk factor for CVD. One of the most significant contributors of SFA to the adult diet is cheese. Despite its high SFA content, cheese intake does not seem to increase the risk of disease (Alexander et al., 2016; O'Sullivan et al., 2013). The mechanisms explaining this paradox has not yet been elucidated but both the high Ca content and other capabilities of the cheese (i.e., ill-defined matrix effects) have been suggested to play a role. Anyhow, it is regarded as a paradox that high cheese intakes do not seem to increase the risk of CVD since high intake of long-chain SFA is consistently associated with a high risk of developing CVD (Hu et al., 1999).

1.6 The role of calcium on lipid digestion

While many articles report a neutral association between cheese and CVD risk, few propose a mechanism as to why this might be the case. An emerging hypothesis has been that of Ca forming insoluble soaps with long-chain SFAs during lipid digestion in the small intestine, reducing their bioavailability and subsequent absorption to the body. Deeper insight into the hypothesis could allow for increased control of what lipids we digest and absorb, which is of interest to the health sector and food- and pharmaceutical industries.

1.6.1 The formation of calcium soaps

Ca plays a vital role in lipid digestion as it alters the interfacial organization of hydrolysed lipids in the fat droplets (Torcello-Gómez et al., 2018). As previously explained, lipids are hydrophobic and thus dependent on forming an emulsion with amphipathic compounds (e.g., bile salts, phospholipids) to travel the aqueous environment of the GI tract. After entry to the small intestine, pancreatic lipase will hydrolyse the TAG molecules in the core of the lipid droplet (Wang et al., 2013). Short- to medium-chain FAs are relatively water-soluble and will leave the fat droplet and be absorbed by the enterocytes. Long-chain FAs are, on the other hand, relatively less water-soluble and will not be able to leave the droplet but instead migrate to the lipid-water interface (Torcello-Gómez et al., 2018). Any endogenous or dietary Ca present in the small intestine will drive the formation of insoluble calcium soaps (CS) with long-chain SFA present at the lipid-water interface at a 1:2 molar Ca to FA ratio. Subsequently, the CS will be removed from the interface by precipitation (Torcello-Gómez et al., 2018). Complexation will only happen when two FFAs are involved (usually SFAs). The precipitation of CS happens when hydrophobic forces arise between several of these complexes (Figure 1.3). MUFAs and PUFAs have branched hydrocarbon chains which will limit efficient precipitation of the soaps. Moreover, longer hydrocarbon chains will create more insoluble soaps. Thus, only long-chain SFAs will create complexes with Ca that readily precipitate. An accumulation of FAs on the interface of the fat droplet will inhibit pancreatic lipase activity as this will restrict the access of lipase to the TAG molecules in the core (Hu et al., 2010). Thus, removing SFA from the droplet interface by CS precipitation will aid the lipid digestion process by leading to faster lipolysis rates (Zangenberg et al., 2001). This is well known in the pharmaceutical industry, as fat-soluble drugs will often have added Ca to aid the uptake of the drugs (Larsen et al., 2011). While lipolysis rates are improved, the FAs that have formed complexes with Ca will be less bioavailable and subsequently be less absorbed (Lorenzen et al., 2007). Additionally, CS formation most likely hinders incorporating the FAs into the mixed micelles (Devraj et al., 2013).

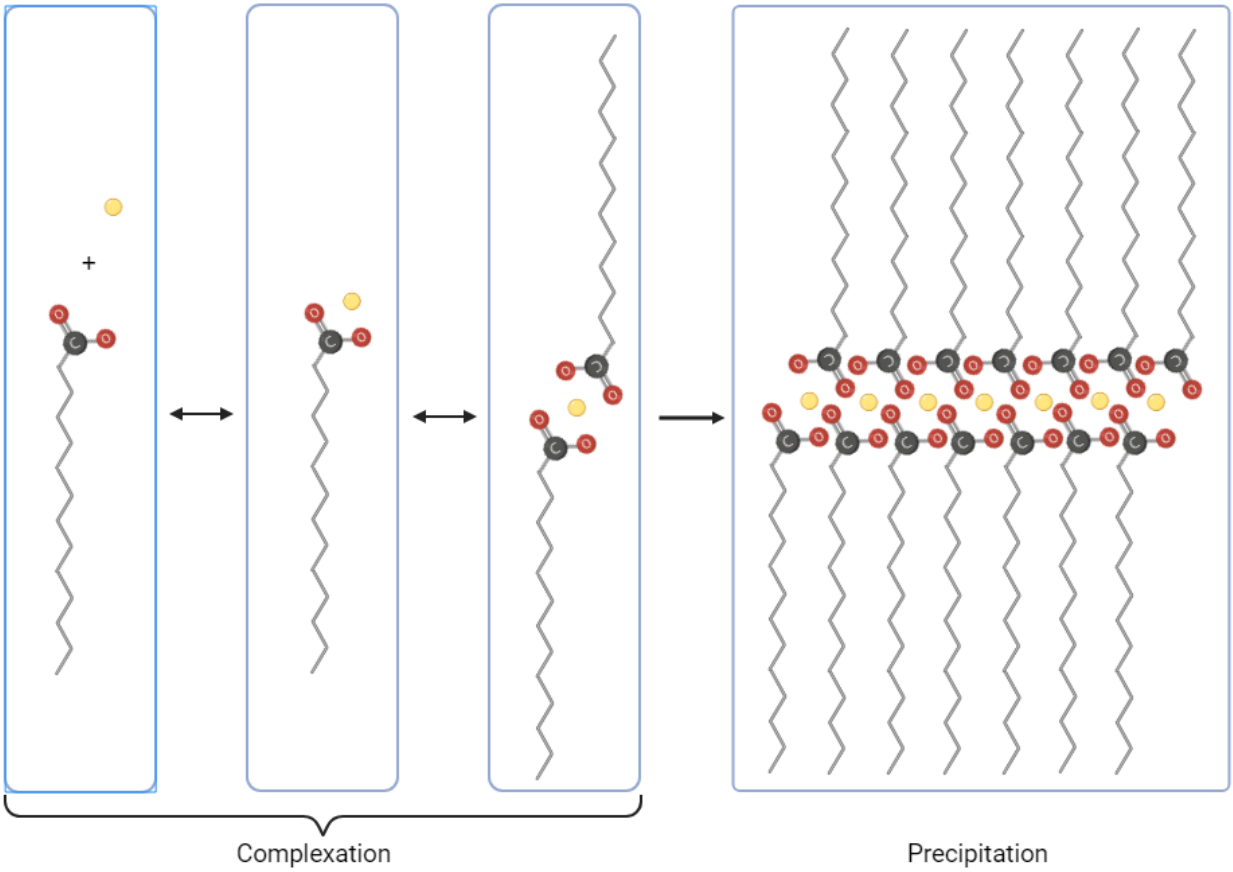

Figure 1.3: Schematic representation of the complexation and precipitation of calcium soaps. Complexation first occurs between one FA and one Ca ion. Another FA will interact with the complex (shown in the third box from the left), a precursor for precipitation. The complex consisting of one Ca atom and two FA can form dimers, trimers and oligomers, driven by hydrophobic interactions, and ultimately precipitate. Ca is shown as a yellow circle, O as a red circle, C as a grey circle. The figure inspired by Pereira and co-workers (Pereira et al., 2012) and is created using BioRender,com. Abbreviations: Ca = Calcium, FA = Fatty acid, O = Oxygen, C = Carbon

1.6.2 Faecal calcium soaps and potential weight loss benefits

If they are not absorbed, the CS should be excreted in the faeces. Still, there is relatively little research on what happens to the CS after precipitation from the fat droplet, and further investigation is required to understand the mechanism fully. Rodent studies have previously been conducted to investigate whether different levels of ingested dietary Ca will impact fat excreted in the faeces (Alomaim et al., 2019; Ayala-Bribiesca et al., 2018). Indeed, both studies showed increased faecal fat excretion in the high Ca groups. However, there is no easy way of directly measuring CS in the faeces. Instead, the most practical approach is to dissolve the CS and measure and quantify the FAs by gas chromatography.

The idea that long-chain SFAs become less available for uptake into the body by Ca complexation and precipitation forms the rationale for this master thesis. If CS are excreted into the faeces, this could have implications for energy intake, weight gain, and obesity-related disease markers.

1.7 The effects of saturated fatty acids on inflammation and barrier integrity

The presence of harmful pathogens or toxic compounds will induce inflammation, which is part of the innate immune response to harmful stimuli. It acts as part of the body's defence mechanism, with the primary objective of removing the potentially harmful intruder and subsequently initiate the healing process (Chen et al., 2017). The induction of the inflammatory responses involves sophisticated signalling pathways that will differ with particular stimuli and body location. However, a general path is usually followed: Pattern recognizing receptors (PRR) on the surface of a cell will react to a stimulus from a pathogen-associated molecular pattern (PAMP), which leads to the induction of inflammatory pathways. Markers of inflammation will be released, which again attracts inflammatory cells to the site of infection (Chen et al., 2017). While inflammation is a rapid and robust immune response, it can cause damage to surrounding tissue. Some damage is acceptable and is easily repaired; however, a shift from short- to long-term inflammation is not desirable and is associated with various diseases (Furman et al., 2019). Intestinal immunity differs from immunity in other organs. The GI tract is constantly under a bombardment of antigens and microbial products derived from both food and microbiota. Should an inflammation be initiated by all foreign molecules, the following battlefield would wreak havoc on the structures of the gut. Thus, the gut has a clear anti-inflammatory presence, with the normal state of the gut being tolerance (Chistiakov et al., 2015).

1.7.1 Saturated fats induce inflammation in the small intestine

Obesity induced by a high-fat (HF) diet feeding has been shown to promote inflammation in the intestine of mice. Wang and co-workers demonstrated that a short-term HF diet increased Toll-like receptor 4 (TLR4) messenger ribonucleic acid (mRNA) expression in intestinal tissues (Wang, N. et al., 2013). Furthermore, the results showed that the TLR4/NF-κB signalling pathway was activated, and an increase was observed over time, peaking at day 7. The primary PAMP of TLR4 is lipopolysaccharide (LPS) present at the external membrane of Gram-negative bacteria (Rogero & Calder, 2018). While LPS is the primary TLR4-ligand, emerging evidence suggests that SFA can act as a ligand (Huang et al., 2012). LPS are composed of a lipid and polysaccharide portion, joined together by an outer and inner core (Steimle et al., 2016). The lipid portion, called lipid A, consists of 6 SFAs with carbon chain lengths of 12-16 carbons. Most likely, certain SFAs can bind and activate TLR4 due to their similarity to the lipid A portion of the LPS molecule (Rogero & Calder, 2018). The TLR4/NF-κB signalling pathway has been shown to initiate the production of pro-inflammatory cytokines, such as tumour necrosis factor-α (TNF-α) and interleukin (IL)-1β, IL-6, IL-8 and IL-12 (Azam et al., 2019; Ko et al., 2011). The cytokines will be able to recruit and activate leukocytes at infection site.

1.7.2 The intestinal barrier

The GI tract consists of an intestinal barrier that separates our bodies from the outside environment and is built up of distinct layers. A mucus layer is the first physical defence against harmful substances in the lumen and is predominantly made up of glycoproteins produced by Goblet cells (Knoop & Newberry, 2018). The small intestine has one mucus layer, whereas the large intestine has two, where commensal bacteria colonise the outer mucus layer (Vancamelbeke & Vermeire, 2017). Underneath the mucus layer(s), a single cell layer of epithelial cells is present. These cells are commonly divided into five types: absorptive enterocytes, mucus-producing Goblet cells, enteroendocrine cells, antimicrobial peptide-producing Paneth cells and microfold cells. The cells are connected with tight junction proteins such as occludins, claudins and zonula occludens (ZO). Tight junction proteins play a crucial part in paracellular permeability as small molecules can travel between the junctions of two cells, while larger molecules usually cannot (König et al., 2016). Underneath the epithelial cells lie the lamina propria, where many activated immune cells are present if any bacteria or pathogens manage to penetrate the barrier (Kamada et al., 2013).

The intestinal barrier possesses conflicting roles: it acts as a semipermeable barrier to absorb nutrients, minerals, and water while simultaneously functioning as a physical and immunological defence barrier against harmful substances. Disruption of the intestinal barrier is associated with many diseases (König et al., 2016), and a breach could cause severe complications.

Diets rich in saturated fats have been shown to reduce barrier function in mice (Lam et al., 2012; Murakami et al., 2016; Suzuki & Hara, 2010). An increased bile flow has been proposed as a mechanism to explain this. HF feeding increases the release of bile from the liver to facilitate fat digestion and absorption. The gall bladder secretes primary bile acids into the duodenum. After aiding in fat digestion, the primary bile acids are absorbed in the jejunum or ileum and transported back to the liver. However, some escape absorption and remain in the intestine, where bacteria modify them to become secondary bile acids which are generally hydrophobic. There is evidence that abnormally high levels of secondary bile acids lead to increases apoptotic epithelial cell death and thus leads to decreased barrier functions (Hegyi et al., 2018). Furthermore, studies in rodents fed a HF diet have reported a down-regulation of tight junction proteins (Cani et al., 2009; de La Serre et al., 2010; Lam et al., 2012), underlining the link between saturated fats and decreased barrier function.

2 AIMS

This master thesis is a sub-project within a larger project called LipidInflammaGenes, a collaboration between NMBU, NTNU (Norwegian University of Science and Technology), UiO (University of Oslo) and TNO (Netherlands Organisation for Applied Scientific Research). The main objective of the LipidInflammaGenes project is to study TAG from Norwegian animal products and how it may affect inflammation and satiety, as well as risk factors of CVD.

The overall aim of the current project was to assess whether the Ca content and/or food matrix could affect the weight development and intestinal health in mice through impacting the amount of SFA uptake and excretion. The food matrices that were compared were cheese and butter containing equal amounts of SFA and otherwise equal in terms of other nutritional content.

We hypothesised that the Ca in the cheese would form insoluble soaps with long-chain SFAs in the small intestine, thus limiting the uptake of these FAs, increase the excretion with the faeces and thus influence the body weight development and intestinal health.

Furthermore, we hypothesised that the food matrix could play an additional role in modifying the uptake of SFA and thus influencing the body weight development and intestinal health.

The project had the following specific aims (**I-IV**):

I. To determine whether Ca impact the FA digestibility and weight development in mice.

II. To determine whether the fat matrix (cheese or butter) influences FA digestibility and weight development.

III. To determine whether Ca and food matrix affects expression of inflammatory and intestinal barrier related genes in the small intestine.

IV. To assess the accuracy of a TD-NMR (time-domain nuclear magnetic resonance) instrument from Bruker on determining body fat in mice.

3 MATERIAL AND METHODS

3.1 Experimental design

3.1.1 Animals and housing conditions

60 male mice of the strain C57BL/6J Rj were used in this experiment. They were ordered from the supplier Janvier Labs in France and shipped to NMBU. The mice were six weeks old at arrival and approximately eight weeks at the start of the intervention. A standard mouse feed (Chow; RM1, SDS Diets, Essex, UK)) was given to the mice for one and a half weeks to acclimatise them to the new environment. During the acclimatisation period, the cages were equipped with bedding, nesting material, houses and running wheels. However, the running wheels were removed from the cages during the intervention to exclude physical activity as a possible confounder. Removal of the running wheels has, from previous experience, also shown decreased fighting between the males. The mice were given *ad libitum* access to water and food.

The mice were housed in individually ventilated cages (Innovive, San Diego, CA) on the same rack. Room lighting followed a 12:12 hour light/dark cycle. A local humidifier (Condair CP3mini, Qviller, Norway) ensured relative humidity to range between 45-55%. The temperature was closely monitored and kept between 23-25 °C.

C57BL/6 is a well-known mouse strain, often used in studies concerning obesity and metabolic syndrome. When put on a HF diet, they will gain weight and develop insulin resistance. Thus, we consider C57BL/6 as a relevant model for the experiment.

3.1.2 Ethical aspects

The animal experiment was approved by The Norwegian Animal Research Authority (Mattilsynet). All procedures complied with the EU's directives on animal research. FOTS ID for the experiment was 25541.

3.1.3 Experimental setup

Male mice (C57BL/6JRj) were fed a HF diet (~45%E from fat) with FAs either from cheese (n=20) or butter (n=30) and received varying Ca levels [low-Ca (2g/kg feed), medium-Ca (7g/kg feed) and high-Ca (20g/kg feed)] for 5 weeks. A control group received a low-fat chow diet with a standard Ca content of 5g/kg (n=10). The mid-Ca cheese feed had no additional Ca added, as the Ca naturally present in the cheese accumulated to 7g Ca/kg feed. Therefore, no low-Ca cheese group was included in the design, as there was no way to reduce the Ca content of the cheese while retaining a comparable matrix. Groups are abbreviated as: chow low-fat control (Chow), butter with 2 g Ca/kg feed (But2), butter with 7 g Ca/kg feed (But7), cheese with 7 g Ca/kg feed (Che7), butter with 20 g Ca/kg feed (But20) and cheese with 20 g Ca/kg feed (Che20) (Figure 3.1).

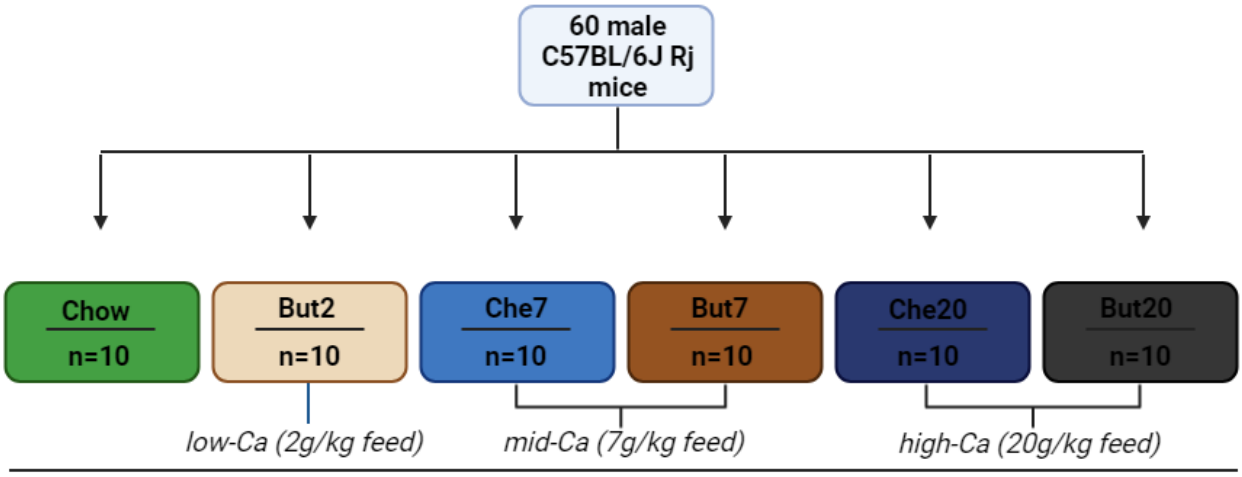

Figure 3.1: Experimental groups. 60 adult male C57BL/6J Rj mice were fed a HF diet with fat from cheese (n=20) of butter (n=30) and received varying Ca levels [low-Ca (2 g/kg feed), medium-Ca (7 g/kg feed) and high-Ca (20 g/kg feed)]. A control group received a low-fat chow diet with a standard Ca content of 5 g/kg (n=10). The figure is created using BioRender,com. Abbreviations: Ca = Calcium, HF = High-fat

Two mice were housed in each cage, and cages were distributed randomly in the cage-racks. Mice are categorised as "social animals", and evidence suggests that individual housing can cause anxiety-or depression-like behaviour in male mice (Kappel et al., 2017). Thus, we decided to house two mice in each cage, maximising the number of experimental units. They were fed their respective diets for five weeks, with detailed timeline of the experiment shown in Figure 3.2. Termination was carried out over five days, with 12 mice terminated each day. The feeding trial started on different days for different animals, corresponding to what days the animals were terminated, to ensure the same length of intervention for all animals.

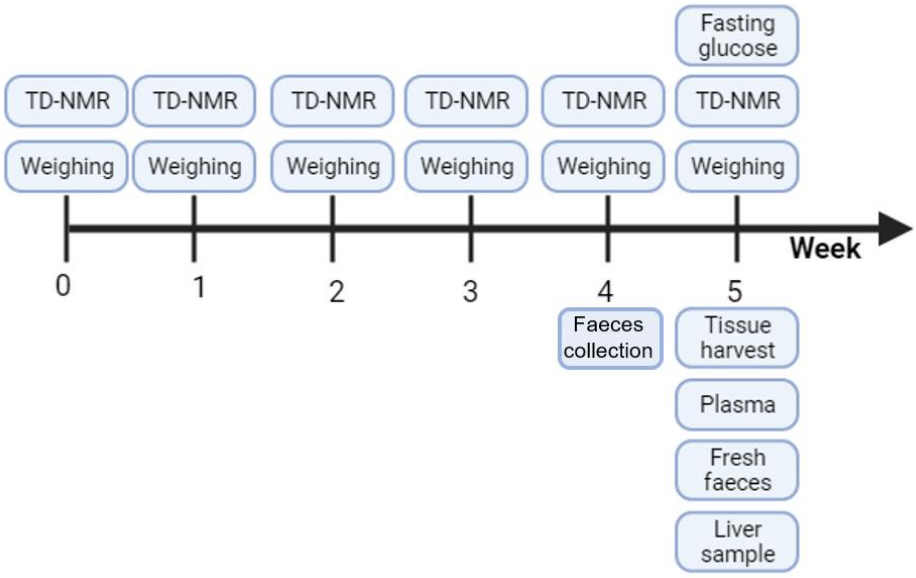

Figure 3.2: Timeline of experiment. The experiment lasted for 5 weeks. Body weight and fat tissue mass (TD-NMR) were measured weekly. Food consumption was monitored weekly (not included in the figure). Faeces were collected every day for one week (week 4). The mice were terminated the fifth week, and tissue, plasma, fresh faeces and liver were collected. Furthermore, the mice were fasted for 4 hours before termination to measure fasting glucose. The figure is created using BioRender,com. Abbreviations: TD-NMR = Time-domain nuclear magnetic resonance

3.2 Mouse diets

All the HF experimental diets were made in-house by mixing all the necessary ingredients and subsequently prepared as pellets. Ingredients were ordered from Dyets Inc. (Bethlehem, PA) with a few exceptions: TINE provided cheese and butter, while casein was made at NMBU. The cheese's fat content had been previously determined at NMBU. Ca was added in the form of Ca phosphate. The HF diets were designed with (D12451, Research diets, New Brunswick, NJ) as a template. The ingredients were adjusted to reach the desired energy composition of 45% fat, 35% carbohydrate and 20% protein. Additionally, the calories were made as similar as possible. The Chow control diet (RM1; SDS diets) was provided as ready-made.

Table 3.1: Compositions of the cheese and butter diets

	Butter 7 g Ca/kg feed		Cheese 7 g Ca/kg feed	
	g%	**kcal%**	**g%**	**kcal%**
Protein	22,65	20.16	22,92	20,00
Carbohydrates	38,80	34,53	39,48	34,45
Fat	22,58	45,21	23,15	45,45
Other (vitamin mix)	1	0,10	1	0,10
Fibre	5,5	0	5,6	0
Total		100		100
Ingredients	**g**	**kcal**	**g**	**kcal**
Cheese			541,7	2638
Butter	239	1787		
Casein	222	888	22,5	90
L-Cystine	3,3	13	3,4	16
Sucrose	196	785	199,9	799
Dyetrose	111	444	112,9	452
Starch	80,8	323	82,2	329
Cellulose	55,5		56,4	
Soybean oil	27,7	250	28,2	254
Mineral mix	38,8		39,5	
Vitamin mix	1,1	4	1,1	4
Choline bitartrate	2,2		2,2	
Calcium phosphate	22,6		0	
Total Ca	7,07		6,73	
Total	**1000**	**4494**	**1000**	**4582**

The diet compositions of Che7 and But7 were chosen as demonstrations of the HF diets. The other HF diets are very similar to those shown in the table, with the main difference being the amount of added calcium phosphate. Abbreviations: HF = High-fat, Ca = Calcium, kcal = Kilo calories.

3.2.1 Calcium considerations and human relevance

Research on the nutritional needs of the rodents led to the AIN-93 rodent diet, which lists the nutritional recommendations of mice and rats (Reeves et al., 1993). They recommend 5 grams of Ca per kilo feed. Mice eat approximately 3 g of food per day, thus consuming ca. 15 mg Ca daily. Humans are recommended to ingest 800-1000 mg Ca/day. To compare the daily intake of Ca between mice and humans, one must consider the difference in metabolic rate between the two species. The total metabolic rate of a 70 kg human is 138 kJ per kg body weight, while the total metabolic rate of a 30 g mouse is 961 kJ per kg body weight (Terpstra, 2001). Hence, the metabolism of mice is approximately seven times faster than that of

humans. The daily Ca recommended intake in mice, adjusted for metabolic differences, should therefore be between 1.5 to 2 mg per day given that no extra Ca is needed for skeletal growth. The low Ca-group (2 g Ca/kg feed) was chosen on this basis.

Our diets were divided into three levels of Ca: low-Ca (2 g Ca/kg feed), mid-Ca (7 g Ca/kg feed) and high-Ca (20 g Ca/kg feed). It would have been natural to make the mid-Ca groups contain 5 grams of Ca, as this matches the recommendations of Reeves and colleagues (Reeves et al., 1993). However, cheese naturally contains Ca. 45% of the energy in the feed came from fat, and cheese accounted for the majority of this. Thus, the natural Ca content of the feed ended up at 7 g per kilo, and it was convenient to make this the mid-Ca level.

The amount of Ca in the high-Ca groups is four times the recommendations of Reeves et al. (Reeves et al., 1993). While this might seem very high, it is crucial to consider the difference in eating habits between mice and humans. Humans eat only a few large meals per day, while mice eat little and often while they are awake. When humans eat large, cheese-filled meals (like pizza), they ingest an amount of Ca and cheese in a time span that could not be easily replicated in a mouse study. An option would be to feed mice with an oral probe (*per oz*); however, this is a very time-consuming process. Instead, we try to simulate the situation in the GI tract of humans straight after a cheese-filled meal by making the mice eat a cheese diet constantly, with high levels of Ca, for 5 weeks.

3.2.2 Cheese preparation

TINE provided a ten-kilo cheese wheel of a nine-month aged cheese called Norvegia Vellagret. NMBU had previously characterised FA composition and mineral content on a selection of Norwegian cheeses. Based on this analysis, Norvegia Vellagret was chosen for its high Ca content, about nine grams per kilo cheese. Upon arrival, the cheese was divided into pieces and then shredded using electrical cheese shredders (Crypto Peerless TRS, UK). Subsequently, the cheese was frozen at -80 °C before being freeze-dried (Heto DryWinner 6-85, Thermo Fisher Scientific, Waltham, MA) for 24 hours to remove as much water as possible. The cheese was then ground to a powder using kitchen machines (Grindomix GM 200, Retsch) and stored at -20 °C.

3.2.3 Casein separation from milk

Casein makes up the majority of cheese protein. Hence, the protein naturally present in Norvegia contributed significantly to the cheese feed's total protein content. In contrast, butter contains very little protein, fulfilling the need to add an external protein source to the butter feed. By isolating and adding casein from Norwegian cows' milk to the butter diet, we ensured the feeds were as similar as possible, as Norvegia would also be derived from Norwegian cattle. The casein was produced in-house at the dairy pilot at NMBU with milk from the NMBU dairy farm (Ås gård).

1M hydrochloric acid (HCl) was added to 100 L of skimmed milk until the pH measured 4.57. The milk was then heated to 42 °C to promote curdling of the casein. The whey was removed and discarded by running the mixture through a filter. Subsequently, the casein was washed in three steps: first, three times with water acidified by sulfuric acid (H_2SO_4) at 42 °C for 15 minutes. Second, the casein was washed three times with acidified water at 38 °C for 15 minutes. Finally, the protein was washed with clean water at 32 °C. The casein was then hung in draining bags for 18 hours at 4 °C to allow excess water to drain. The following day, the casein was cut up and portioned into sealed plastic bags for storage at -20 °C.

3.2.4 Casein analysis

Dry matter and Ca analysis were performed on the casein to evaluate water content and Ca levels. The Ca analysis was critical, as "unregistered" Ca could impact fat uptake and disrupt results.

5 g of casein was weighed in three parallels for both the dry matter and casein analysis. The casein designated for the dry matter analysis was put in aluminium foil cups, while the casein for the Ca analysis was put in heat resistant porcelain crucibles. The cups and crucibles were carefully weighed before the addition of casein. The samples were placed in an oven at 100 °C for 24 hours to ensure complete evaporation of the water present. Water content was calculated by dividing the dry sample's weight with the weight of the wet sample.

For the Ca analysis, the porcelain crucibles were transferred to a muffle oven, and the temperature was set to 650 °C. The samples were checked regularly and removed from the oven when all material was turned into white/grey ash, which required approximately 6 hours. Some drops of HNO_3 were added after 3 hours to aid the ashing process.

10 mL of 1M HCl was added to each crucible, and a glass stick was used to homogenise the solution. The solution was then transferred to 200 mL measuring flasks, and distilled water was added to the 200 mL mark. Subsequently, 25 mL of solution was transferred to an Erlenmeyer flask, and 20 mL of buffer solution was added. A spatula point of Erichromeblack T was added to give a dark red/violet colour. Ethylenediaminetetraacetic acid (EDTA) was added drop by drop to the solution until a stable blue colour appeared. The amount of EDTA titrated was noted and used to calculate the amount of Ca in the original casein sample. The formula used for calculating Ca in casein is given in (1).

$$\%\ \boldsymbol{Ca\ in\ casein} = \frac{mL\ used\ EDTA * factor^{1} * 8^{2} * 100}{mg\ weighed\ casein} = \frac{mL\ used\ EDTA * 0.4 * 8 * 100}{mg\ weighed\ casein} \quad \textbf{(1)}$$

[1] The factor is 1/EDTA the strength of the solution. 1 mL EDTA corresponds to 0.4 g Ca^{2+} and the strength of the EDTA solution is thus 2.5. The factor is then 1/2.5 = 0.4

[2] Dilution factor

Abbreviations: Ca = Calcium, EDTA = Ethylenediaminetetraacetic acid

3.2.5 Preparing the mouse feed

Ingredients for the mouse feed were separately weighed and added to a mixing bowl. Dry ingredients were first mixed to ensure proper homogenisation before the liquids were added. Additional water was added to the cheese mixture to make it more easily mouldable. In contrast, the butter mixture was very wet due to the added casein's high water content. Ingredients were mixed in an industrial food processor using the dough hook attachment. The batter was then made into pellets by filling up 25 mL syringes with sawed-off tips. The piston was used to push the batter out, creating a compact "sausage". Subsequently, the sausages were divided into pellets using the chow pellet size as a guide. The pellets were frozen at -80 °C before being freeze-dried for 24-48 hours (Figure 3.3). The butter pellets contained more water than the cheese pellets and were freeze-dried for approximately twice as long as the cheese pellets. The feed was stored at -20 °C until the intervention started.

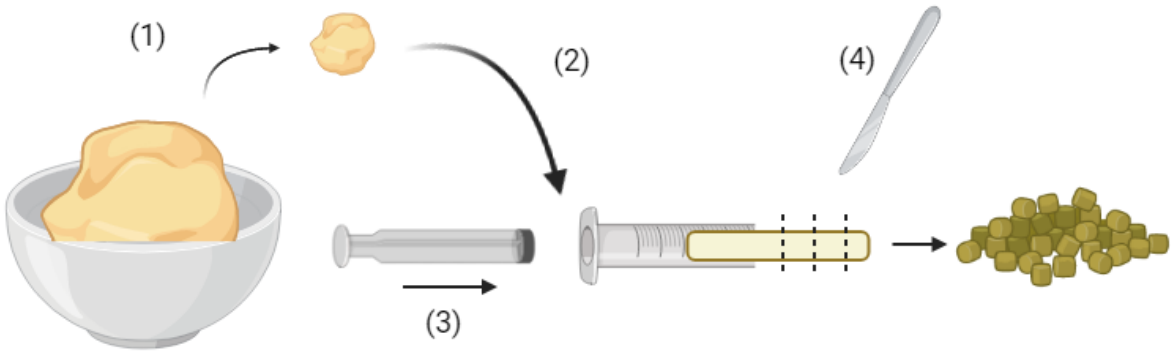

Figure 3.3: Illustration of how the pellets were made. (1) All ingredients were first mixed in a mixing bowl. **(2)** The batter was put into a syringe with a sawed-off tip, making it as compact as possible. **(3)** Subsequently, the syringe's piston was used to push the batter out where it was cut **(4)** into appropriately sized pellets. The pellets were freeze-dried to remove water. The figure is created using BioRender,com.

3.3 Food intake and weight development

Food intake and weight development were monitored closely. Mice were weighed at baseline and subsequently once a week until termination. The mice were given *ad libitum* access to the food, which was refilled once a week. The food was weighed before it was given to the mice. A week later, the remaining food was weighed and subtracted from the original amount to estimate the food intake. The estimate was divided by the number of mice in the cage.

3.4 Sample harvesting

3.4.1 Faeces collection

Faeces were collected for one week to calculate % digestibility and analyse the faecal fat content. As the intervention was initiated and terminated on five consecutive weekdays, the faeces collection was structured similarly. For example, the 12 mice that started the intervention on a Monday had their faeces collected from Monday to Monday. The mice that started their intervention on a Tuesday had their faeces collected from Tuesday to Tuesday, and so on.

At the start of the collection process, the mice were transferred to new cages. The bedding was not replaced due to the difficulty in separating the faeces from the bedding. Instead, a blue paper was placed at the cage's base, making the surface softer for the mice in the absence of bedding. The cage was subsequently enriched with old and new nesting paper, housing and wooden sticks.

To collect the faeces, mice, housing, sticks and paper were removed from the cage. The paper was thoroughly checked as faeces would often stick to it. A forceps was utilised to pick up faeces and place them in marked falcon tubes. When all faeces were collected from the cage, the falcon tube was weighed and stored in the freezer at -20 °C. The cage was wiped to remove hair, urine and water before a new piece of blue paper was laid at the cage's bottom. The mice were reintroduced to the cage together with sticks, paper and housing. The routine was repeated every day for all cages.

Additionally, faeces were collected from the mice on the day of the termination. The mice were put in empty containers and allowed to defecate. Subsequently, the faeces were picked up with clean forceps and placed in Eppendorf tubes. The tubes were flash-frozen in liquid N_2 to preserve the samples.

3.4.2 Blood collection and plasma preparation

During the termination of the animals, blood was sampled by cardiac puncture. The animals were fully anaesthetised by intraperitoneal injection of a ZRF-cocktail (ca. 10 µL/g mice). The cocktail is a mixture of Zolazepam, Xylazine, Fentanyl and Tiletamine, achieving anaesthesia and analgesia. A 1 mL syringe with a 25-gauge needle was inserted below the rib cage, through the diaphragm and into the heart. Between 0.5-1.2 mL of blood was extracted to Eppendorf tubes. EDTA was used as an anticoagulant. Animals were subsequently sacrificed with cervical dislocation. Blood was kept on ice until all samples were collected and centrifuged (6000 g, 4 °C) for 10 minutes to separate red blood cells and plasma. A pipette was used to transfer as much plasma as possible to a new tube without contamination of red blood cells. Plasma was stored at -80 °C, awaiting analysis. Blood was sampled with the intent of analysing insulin levels. However, due to time restrictions, insulin analysis was not performed during this master project.

3.4.3 Mucosa from the small intestine

After cervical dislocation, mice were prepared for dissection. Mice were pinned down on a sterile plate, and the abdomen was sprayed with ethanol before it was opened. The intestine was removed and washed in phosphate-buffered saline (PBS), then transferred to a disinfected plate. The duodenum, jejunum and ileum were identified and isolated. Mucosa was harvested by cutting the intestine longitudinally and using a blunt microscope slide to scrape along the intestine. Immediately after, mucosa was transferred to Eppendorf tubes containing 200 µL of RNA*later* (RNAlater, Thermo Fischer). Tubes were left in the fridge at 4 °C for 24 hours to allow RNA*later* to properly penetrate the mucosa before being stored at -80 °C, awaiting gene expression analysis.

3.4.4 Liver and epidydimal fat

The left liver lobe was removed from the carcass, and a sample of 20 mg was cut from the distal part. It was immediately transferred to an Eppendorf tube containing RNA*later* (200 µL) and placed in the fridge at 4 °C for 24 hours. Subsequently, the samples were stored at -80 °C. The remaining part of the left lobe was flash-frozen in N_2 and stored at -80 °C. Another master student performed liver gene expression analysis, and the results are not included in this thesis.

Furthermore, a piece of epidydimal fat was harvested and flash-frozen in liquid N_2 and stored at -80 °C. Analysis of the epidydimal fat was not performed during this master project.

3.5 Analysis of fat in feed and faeces

We hypothesised that the formation of CS in the small intestine will reduce the uptake of FFAs from the diet. If the fat is not taken up during digestion, its destination should be in the faeces. By comparing the fat intake of the mouse to how much fat it excreted, it is possible to calculate how much fat is taken up into its body, known as % digestibility. The formula for % digestibility is given in (2).

$$Fat\ digestibility\ (\%) = \frac{Fat\ consumed - Fat\ in\ faeces}{Fat\ consumed} * 100 \quad \textbf{(2)}$$

Thus, we wanted to quantify the amount of fat in the feed and faeces of the mice. Furthermore, we wished to look at individual FAs. This was done by first extracting the total lipids from the feed and faeces. Second, the lipids were fractionated into FFA and neutral lipids (NLs) (i.e., TAG, DAG and MAG) by solid-phase extraction (SPE). Third, the FFA and NL were converted into fatty acid methyl esters (FAME). Finally, the individual FAMEs were separated based on boiling point by gas chromatography–mass spectrometry (GC-MS) (Figure 3.4).

Figure 3.4: Flow diagram of fat extraction and analysis. The figure shows the methods used to extract the fat in feed and faeces, ending with the calculation of % digestibility. The figure is created using BioRender,com.

3.5.1 Lipid extraction and separation

Extraction of total lipids from faeces and feed was performed using the Folch lipid extraction method (Folch et al., 1957). The method was initially designed to extract total lipids from tissue but has proven itself effective on other biological samples. Jordi Folch's lipid extraction method was published in 1957 but has withstood the test of time and is today, together with the Bligh and Dyer method, considered the gold standard of lipid extraction (Breil et al., 2017).

500 mg of frozen faeces or feed were homogenised using an analytical mill (IKA A11 basic) and placed in plastic Falcon tubes (50 ml). 20 mL of 2:1 chloroform:methanol was added to the tubes. One Falcon tube was left free of sample and acted as a control. A control sample was essential as chloroform could dissolve some of the plastic in the tubes, which contains FAs. 300 µL TAG internal standard (IS) 19:0 (100 mg/mL) (Larodan, Monroe, MI, USA) was added to the feed samples. In the faeces samples, 220 µL of FFA 19:0 IS (10 mg/mL) (Larodan, Monroe, MI, USA) and 15 µL of TAG 19:0 IS (10 mg/mL) (Larodan, Monroe, MI, USA) were added. HCl was applied drop by drop to all the Falcon tubes containing faeces until the pH was below 2 (checked with pH strips). The samples were acidified to dissolve any CS present. Acid was not added to the feed samples as there should be no CS present in them. All Falcon tubes were placed on a shaker for 20 minutes at room temperature. The samples were washed with 4 mL saline and centrifuged at 2000 rpm for 30 minutes. After centrifugation, the top layer of methanol (water phase) was discarded. The bottom phase (chloroform) containing the lipids were extracted with glass pipettes and run through filters (Millex-FG hydrophobic PTFE membrane filters, 0.2 µm pore size and 25 mm diameter) to marked glass tubes. The chloroform was evaporated using an evaporator (Sample Concentrator SBHCONC/1, Stuart) running on nitrogen for 1-2 hours.

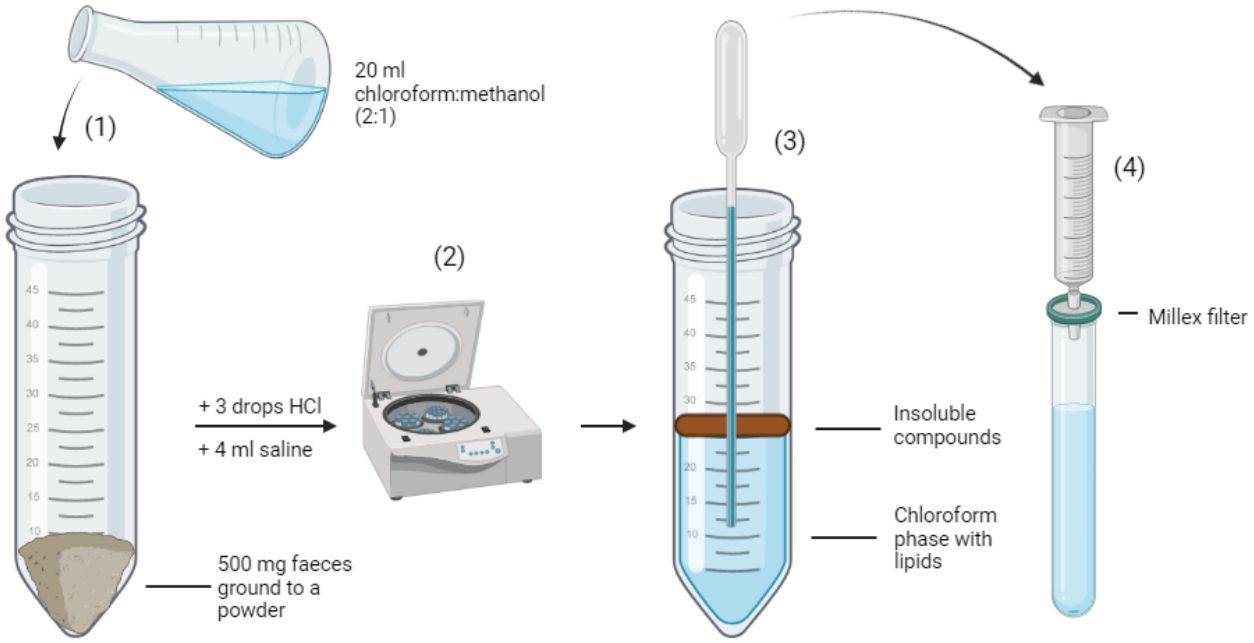

Figure 3.5: Folch extraction and filtration of lipids. 500 mg of frozen faeces was ground to a powder and placed in a Falcon tube. **(1)** 20 mL of 2:1 chloroform:methanol, internal standards (not shown) and 3 drops of 4M HCl were added to the tube and shaken for 20 minutes. 4 mL of saline was added before the tubes were **(2)** centrifuged for 30 minutes at 2000 rpm. After centrifugation, the top aqueous phase was removed and discarded before the **(3)** pipette was carefully inserted through the phase of insoluble compounds. **(4)** Chloroform containing the lipids was poured into a syringe with a Millex filter attached to remove any large particles. The figure is created using BioRender,com. Abbreviations: HCl = Hydrochloric acid

3.5.2 Isolation of FFA and NL by solid-phase extraction

SPE provides the opportunity to isolate the lipids into fractions of FFAs, NLs and polar lipids (e.g., phospholipids). Furthermore, it is possible to divide NLs into TAG, DAG and MAG; however, that was not done in this project. Fractioning by SPE is not required to run the samples on GC-MS, as it is entirely possible to convert the total fat extracted to FAMEs. However, by fractionating into FFAs, NLs and polar lipids, it is possible to determine how much the fractions contribute to the total fat content. We decided to include SPE in our analysis as it increases the specificity of the information provided. Ca only makes complexes with FFAs, which makes this fraction of particular interest. Furthermore, we decided to only fractionate into FFAs and NLs. While there are some phospholipids in the feed, evidence suggests that bacteria highly influence the phospholipids in the faeces (Davies, 2014), thus making the fraction of little interest to us.

The concentrated lipids were resuspended in 1 ml of chloroform and transferred to brown GC-vails with a screw cap. Vials were placed in the SPE instrument (GX-274 ASPEC system, Gilson Inc.), where chloroform was used to extract NLs, while a mixture of ether and acetic acid (98:2) was used to extract FFAs. Before the run, iso-Propanol was used to clean the system and ensure that no air bubbles were

present in the tubes of the instrument. During the run, heptane was used as a cleaning solvent. Columns (Discovery™ DSC-NH2, Supelco™, PA, USA) were placed in the instrument, and the program was started. SPE was only performed on the faeces samples.

3.5.3 Derivatisation of lipids

Derivatisation of the lipids is necessary before they are injected into the GC-MS. There are two primary reasons for this: First, derivatisation converts heat-stable compounds with low volatility into more volatile compounds that can be analysed in a gaseous state. Second, the derivatisation of FAs creates nitrogen derivates, making it possible for the GC-MS to detect where double bonds are located on the hydrocarbon chain of the FA (Řezanka et al., 2016).

The lipids extracted from the feed were converted to FAMEs using a combined method of transesterification and esterification. After evaporation of the chloroform, lipids were dissolved in 1 mL heptane. The glass tubes were heavily vortexed to homogenise the solution. 1 mL of sodium methoxide (5 mg/mL) was added, and the tubes were put on a shaker at 390 rpm for 20 minutes. The sodium methoxide solution was prepared by adding 2.5 mg of metallic sodium (Purum, Merck, Darmstadt, Germany) to 50 mL of methanol. 1 mL of 10-14% BF_3-methanol was added, and the tubes were placed on a water bath at 80 °C for 20 minutes. The tubes were removed from the water bath and cooled to room temperature before being centrifuged at 2000 rpm for 5 minutes. The top layer of the solution was removed to gas chromatography (GC) vials. Furthermore, the feed samples were diluted at 1:100 in heptane before injection into the GC-MS.

After evaporation of the chloroform, the NLs extracted from the faeces were resuspended in 2 mL heptane. 1.5 mL of a 3.3 mg/mL solution of sodium methoxide was added to each sample. The samples were shaken for 30 minutes before centrifugation at 2000 rpm for 5 minutes. The top heptane layer was transferred to GC vials and diluted in heptane at 1:5.

The ether and acetic acid were first evaporated before 1 mL of BF_3-methanol was added to the FFA samples. They were placed in a water bath at 80 °C for 5 minutes before being allowed to cool down to room temperature. 1 mL of heptane was added, and the tubes were heavily vortexed. Next, the samples were centrifuged at 2000 rpm for 5 minutes before the top layer was removed to GC vials. The samples were diluted at 1:10 in heptane.

3.5.4 GC-MS

GC is used for chemical analysis, where compounds are vaporised without being decomposed. It can be used as a means for compound separation, identification and purification. The compound in question will be dissolved in a solvent, for instance, heptane or toluene. The liquid is injected into the instrument. An

inert carrier gas, often hydrogen or nitrogen, will carry the compounds into the column. The carrier gas acts as the "mobile phase". The walls of the column are covered in a liquid which acts as the "stationary phase". Compounds will interact with the stationary phase differently, depending on their boiling points and size, thereby having different retention times. The temperature in the column is high, and the compounds will thus be vaporised. How fast this happens depends on the boiling point of the compound. A low boiling point causes the compound to readily vaporise and travel quickly through the column, while a high boiling point causes longer retention times.

After the NLs and FFAs had been converted to FAMEs, they were run on a GC-MS. 1 µL of the sample was injected into the injection chamber at 250 °C in split mode, with a split ratio of 1:10. The split flow was set to 10.0 mL/min, and the purge flow was set to 5.0 mL/min. The GC used was a TRACE™ 1310 (Thermo Fisher Scientific, Waltham, MA, USA), equipped with a 60 m Rtx®-2330 capillary column with ID 0.25 mm and 0.20 µm film thickness (Restek, Bellefonte, PA, USA). The inert carrier gas used was helium (99.99990%, AGA, Norway), set at a constant flow of 2.0 mL/min. Furthermore, the GC was connected to an AI/AS 1310 Series Autosampler, thus relinquishing the need to place each GC-vial manually. The GC oven temperature was programmed and is shown in Table 3.2.

Table 3.2: Temperature program for the GC-MS oven

Time (min)	Temp. increase rate (°C/min)	Temperature (°C)	Holding time (min)
5	0	50	5
35	100	140	30
65	10	145	30
95	3	175	20
108	50	260	10

The GC oven temperature started at 50 °C for 5 min before it was increased with a rate of 100°C/min to 140 °C, where it was held for 30 min. Subsequently, the temperature was increased to 145 °C at a rate of 10.0 °C/min for 30 min, before being further increased to 175 °C at a rate of 3 °C/min for 20 min. Finally, the temperature was increased at a rate of 50 °C/min to the highest temperature of 260 °C and held for 10 min. The total run time of each sample was 108 min. Abbreviations: GC-MS = Gas chromatography–mass spectrometry Temp = Temperature, Min = Minutes.

The detector on the GC was a mass spectrometer ISQ™ QD GC-MS (Thermo Fisher Scientific, Waltham, MA, USA) that breaks down the molecules into ionised fragments, which are detected by their mass-to-charge ratio. Thus, it can identify and quantify the FAMEs present in the samples. The MS was a single quadrupole, using an electron ionisation energy of 70 eV. The mass range was *m/z* 50 – 450, and full-scan acquisition mode was used with 0.2 sec scan time. The MS transfer line and ion source were both set at 250 °C.

The software used for the analysis was Chromeleon v7.2.9 (Thermo Fisher Scientific, Waltham, MA, USA). 37 FAMEs (Food Industry Fame Mix, Restek, Bellefonte, PA, USA) were used as external standards to verify the FAMEs identified by the MS. Furthermore, the FAMEs in the samples were quantified using the amount of IS added together with predetermined relative response factors. The formula used for quantification of FAME is given in (3). Unknown peaks in the chromatogram were compared to a reference library (NIST 17 Mass Spectral Library, Gaithersburg, MD, USA) for identification.

$$C_{FAME} = \frac{A_{FAME} * C_{IS}}{A_{IS} * RRF} \quad \textbf{(3)}$$

Abbreviations: C = Concentration, A = Area, FAME = Fatty acid methyl ester, IS = internal standard, RRF = relative response factor.

3.5.5 Method development and optimisation steps

During a trial run of the fat extraction and analysis method, faeces samples were run of the GC without being filtrated first. The samples contained large particles, which clogged the system and caused chromatograms that could not be analysed. Thus, a filtration step was added after the Folch extraction to remove larger particles that were not lipids. The filters used were the 0.20-micrometer pore size, 25 mm diameter, Millex-FG hydrophobic PTFE membrane filters. They were chosen due to Teflon's high resistibility to chloroform.

The samples were centrifuged at 2000 rpm for 30 minutes instead of 5 minutes as the original protocol demanded. After 5 minutes of centrifugation, visible particles were floating in the water and fat phase. The additional centrifugation time helped solidify the phases.

The first test runs of the method were executed on a GC with a flame ionisation detector (FID). The GC-FID seemed the appropriate instrument as similar experiments had used it to identify fat in faeces (Alomaim et al., 2019; Ayala-Bribiesca et al., 2018). However, a problem arose when 37 external standards were run on the GC-FID, and some peaks could not be identified. The identification problem was most likely due to the manufacturer using a different column than us, which caused the retention times to differ. Thus, we decided to use a GC-MS instead. The advantage of an MS is that it utilises mass spectrometry to identify the FAMEs. Furthermore, it is equipped with a reference library where unknown peaks can be looked up. While a set of external standards is also run on the GC-MS, they are used to double-check the peaks in the samples, rather than being the sole source of identification (i.e., GC-FID).

An IS is used to quantify each FAME present in the sample. The amount of IS added should be relevant to how much fat is in the samples (i.e., the IS peak should not be vastly different from the other peaks in the

chromatogram). The amount of fat in the feed was known (as well as individual FAs). Hence the appropriate amount of IS to add could be calculated. However, the amount of fat in the faeces was unknown, so a pilot was performed to determine how much IS should be added to the faeces samples. Based on the pilot results, 15 µL of TAG 19:0 and 220 µL of TAG 19:0 was found to be within the relevant ranges.

A high concentration of the FAMEs causes large peaks on the chromatogram, which can clump together, making the analysis difficult. The feed samples were abundant in fat and were thus diluted at 1:100 with heptane before injection to the GC-MS. The faeces samples were diluted at 1:10 with heptane.

3.6 RNA extraction

During termination of animals, liver tissue and gut mucosa were sampled for gene expression analysis. Due to the mRNA's fragile nature, the samples were stored in Eppendorf tubes containing 200 µL of RNA*later* to prevent mRNA degradation. Samples were first stored in the fridge at 4 °C for 24 hours, as the manufacturer recommends (RNAlater, Thermo Fischer), to ensure proper tissue penetration. Subsequently, the samples were stored at -80 °C until the extraction was performed.

The NucleoSpin RNA/Protein Kit was used to isolate the RNA. The kit utilises a spin basket format, where the lysate is passed through a derivatised silica gel membrane that will bind nucleic acids. Subsequently, the membrane is washed in several steps before the RNA is eluted into collection tubes.

The procedure was executed following the manufacturer's protocol (Machery-Nagel, 2014). A maximum of 30 mg of gut mucosa was weighed and put in tubes. 350 µL of RP1 Buffer and 3,5 µL of β-mercaptoethanol (β -ME) was added to the tissue. A 1 mL syringe with a 25-gauge needle was utilised to homogenise the sample. The solution was injected and ejected through the needle until the desired texture was accomplished. When introduced to the RP1 buffer, the cells will undergo lysis due to the presence of guanidine thiocyanate. The guanidine salts also act as an RNase inhibitor, thus protecting the exposed RNA. β -ME acts as a reducing agent, breaking the disulfide bonds of the proteins.

The lysate was transferred to a NucleoSpin filter connected to a collection tube and centrifuged at 11000 x g for 1 minute. The purpose of the filtration was to reduce the viscosity of the lysate as well as clearing it. After centrifugation, 350 µL of ethanol (70%) were added to the collection tube to adjust the RNA binding conditions. The samples were vortexed to ensure proper homogenisation of the solution.

The samples were loaded into the NucleoSpin RNA/Protein columns, placed in collection tubes, and centrifuged at 11000 x g for 30 seconds. The nucleic acids will bind to the silica gel column, thus isolating RNA (and DNA) while the proteins will flow through. As we are only interested in RNA isolation in this experiment, the flowthrough was discarded, and the columns were put in new collection tubes. 350 µL of

Membrane Desalting Buffer (MDB) was added to the columns, followed by centrifugation at 11000 x g for 1 minute. Desalting the silica membrane is done to enhance the effectiveness of the rDNase, an enzyme that degrades DNA. The rDNase reaction mixture was prepared in a sterile microcentrifuge tube by adding 10 µL of rDNase to 90 µL of Reaction Buffer for rDNase for every sample. Subsequently, 95 µL of the reaction mixture were added to the columns, and they were left to incubate at room temperature for 15 minutes.

The silica membrane gel was then washed and dried in three steps. During the first wash, 200 µL of Buffer RA2 was added to the columns to inactivate the rDNase, followed by centrifugation for 30 seconds at 11000 x g. The columns were put into new collection tubes. Any leftovers of the RA2 Buffer were washed away during the second wash by adding 600 µL of RA3 Buffer and centrifuging at 11000 x g for 30 seconds. The flowthrough was discarded, and the columns were placed in the same collection tubes. During the third wash, 250 µL of RA3 Buffer was added to the columns, and centrifugation commenced for 2 minutes at 11000 x g to ensure a dry membrane.

Flowthrough was discarded, and the columns were put in RNase-free collection tubes. To eluate the RNA, 60 µL of RNase-free water was applied to the columns, followed by centrifugation at 11000 x g for 1 minute. The isolated RNA present in the collection tubes was collected and analysed to evaluate concentration, degree of purification and integrity.

3.7 RNA quality and quantification

NanoDrop spectrophotometer was used to assess the quality and quantity of the isolated RNA. RNA will absorb light at 260 nm, and by utilising the Beer-Lambert law, the concentration of RNA was predicted. The Beer-Lambert law predicts that a solution's absorbance is directly proportional to the absorbing species' concentration (Mayerhöfer et al., 2020). Thus, a reading of 1 at A260 would be equivalent to 40 µg/mL mRNA. Additionally, absorbance at 230 and 280 nm was investigated to evaluate the purity of the isolated RNA. Proteins will absorb wavelengths up to 280 nm, and a low A260/A280 ratio could indicate protein contamination. A low A260/A230 ratio could indicate other contaminants, such as leftover guanidine from the RP1 Buffer. Ratios between 1.7-2.1 were accepted as highly purified RNA and acceptable for gene expression analysis.

It is essential to assess the RNA samples' integrity, as degraded RNA would cause problems during complementary DNA (cDNA) conversion and, subsequently, the gene expression analysis. The assessment was done using the Agilent 2100 bioanalyzer and the Agilent RNA 6000 Nano Kit. The instrument utilises a combination of capillary electrophoresis and fluorescent dyes to evaluate RNA concentration and integrity. The software 2100 Expert will analyse the capillary electrophoresis results and calculate an RNA

integrity number (RIN) between 1 and 10. A low RIN-score indicates a high degradation of the sample, while a high RIN-score indicates an unimpaired sample.

3.8 Gene expression analysis with quantitative real-time PCR

3.8.1 cDNA synthesis

Gene expression analysis by real-time polymerase chain reaction (PCR) is dependent on DNA. Therefore, cDNA synthesis from RNA using the iScript cDNA Synthesis Kit was performed following the supplier's instructions (BioRad). The kit utilises a modified reverse transcriptase (RT) derived from a Moloney murine leukaemia virus (MMLV). RT will bind to the RNA-template and begin the synthesis of a single cDNA strand. The reaction mix contains random hexamer primers and oligo(dT), which are essential for the RT's function. RNase H will then degrade the RNA-template, leaving single-stranded cDNA that can be amplified during real-time PCR.

3.8.2 Quantification by real-time PCR

PCR was discovered in 1983 and is an *in vitro* method of amplifying a DNA fragment. Several variants of the traditional PCR have been made, among these: Real-time PCR. Real-time PCR, also known as quantitative PCR, allows for quantitative measurements of nucleic acids during PCR. It has become an important tool in gene expression analysis.

PCR is a method for amplification of a DNA target sequence. It involves three steps: denaturation, annealing and extension. During denaturation, the temperature is set at 94 °C that will cause double-stranded DNA (dsDNA) to denature. Creating single-stranded DNA (ssDNA) is vital for the method as it allows for primer hybridisation during the annealing step. The temperature is reduced to 55-70 °C as specific forward and reverse primers bind to ssDNA's flanks. During extension, a heat-stable DNA polymerase will bind to the DNA strand at 72 °C. It will synthesise dsDNA, utilising the deoxyribonucleotide triphosphates (dNTPs) present in the system. As shown in Figure 3.6, the first step involves a linear ground phase (1) as the reaction gets going. An exponential phase (2) is initiated when the target sample is doubled for each PCR cycle. During the log-linear phase (3), the reaction takes place at a linear efficiency. Towards the end of the reaction, reactants become limited, and a plateau phase (4) is initiated as target DNA amplification is reduced.

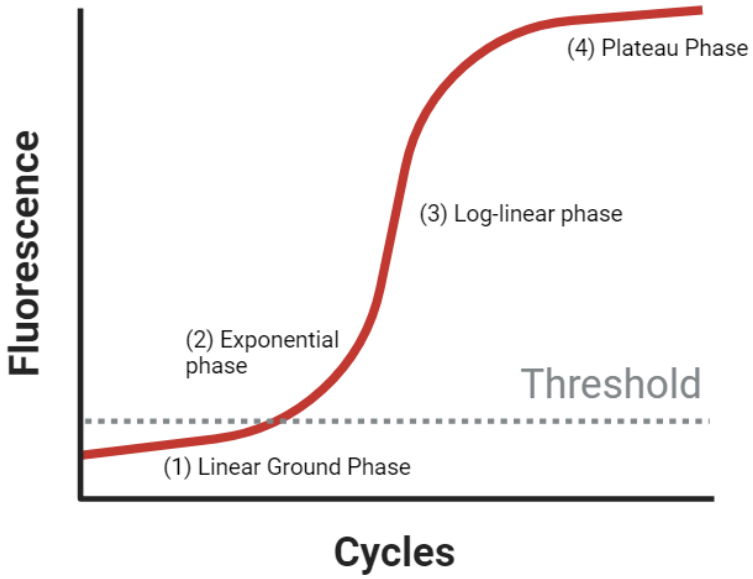

Figure 3.6: The four phases of real-time PCR. Fluorescence is plotted versus cycles. **(1)** shows the area of the curve in the beginning of a PCR run emitting fluorescence below the threshold, **(2)** is the exponential phase of the PCR reaction, as the product is doubled at each cycle, **(3)** visualise the log-linear phase of the reaction where it occurs at a linear efficiency, whereas the plateau phase **(4)** is when the components of the reaction is limited and the amplification is reduced. The figure is inspired by Yilmaz et al. (Yilmaz et al., 2012) and is created using BioRender.com. Abbreviations: PCR = polymerase chain reaction The figure is created using BioRender,com.

Real-time PCR utilises fluorogenic dyes as a mean of sequence non-specific detection. SYBR Green I is the most frequently used dye in Real-time PCR. When unbound, SYBR Green I will emit a low level of measurable background fluorescence. However, in the presence of dsDNA, the dye will bind to the minor grooves of the dsDNA. Bound SYBR Green I emit fluorescence a thousand times stronger than unbound SYBR Green I. As the target DNA is amplified, there will be more opportunities for the fluorescent dye to bind dsDNA. The fluorescence is measured by the quantitative PCR instrument and will be proportional to the amount of dsDNA present.

During the early PCR cycles, the emitted fluorescence from bound SYBR Green I will not surpass the background level and will not be detectable. However, during the exponential phase, the bound dye's fluorescence will reach a threshold where it overcomes the background fluorescence. This is known as the cycle threshold (Ct). Samples containing low amounts of initial target DNA will use more cycles to reach the Ct than samples with a higher initial material amount.

3.8.3 Analysis of gene expression

The software LinRegPCR was used to calculate the Ct value for each sample. It utilises a method called relative quantification that determines the changes in steady-state mRNA in response to different treatments (Yilmaz et al., 2012). The gene of interest is compared to an internal RNA control, usually a

housekeeping gene (HKG). HKGs are expressed at relatively constant rates in all cells. Relative quantification does not measure mRNA concentration (absolute quantification) but looks at the target gene's mRNA expression levels relative to the reference gene. In our case, the reference gene chosen was glyceraldehyde 3-phosphate dehydrogenase (GAPDH).

Amplification efficiency is a term that describes how well the target sequence is amplified during the exponential phase. An amplification efficiency of 1 would be equivalent to 100% efficiency as the target sequence is doubled for each cycle. It is crucial to evaluate this as a slight difference in amplification efficiency between the target gene and reference gene could cause significant differences when calculating expression ratios (Yilmaz et al., 2012). Nevertheless, a slight margin of error is accepted, and amplification efficiencies between 90-110% are generally considered sufficient (Tichopad et al., 2003). Furthermore, using the Pfaffl model for relative quantification, a correction is made for amplification efficiency. Pfaffl created a mathematical formula that combined gene quantification and normalisation of the target and housekeeping gene's amplification efficiency (Pfaffl, 2001). The software LinRegPCR was used to check if the genes' amplification ratios were within the accepted range.

3.9 TD-NMR for determining fat content in live mice

The protons of hydrogen will have a positive charge of +1, a property known as nuclear spin. Usually, the nuclear spin of the protons will be randomly oriented. However, within a magnetic field, the hydrogen nuclei's orientation will either be with or against the magnetic field, a phenomenon known as polarisation. A pulse will induce excitation of the protons, causing the spin to be angled perpendicular to the magnetic field. With time, the protons will return to their original orientation, known as relaxation. The relaxation time will be different for protons in different matrices, thus creating the ability to differentiate between fat, lean mass and free fluids.

Fat tissue mass was analysed using the Minispec LF50 (Bruker, Billerica, MA). Magnet temperature was set at 37 °C, while proton frequency was 7.5 MHz. The instrument was checked and cleared before sample measurement. This was done by inserting a standard sample (chia-seeds) with known quantities of fat and running the "daily check" command. Sample batch, calibration type (mice 5-60 g), mouse-ID and weight were specified for all animals. The mouse was picked up by the root of its tail and placed in a red plastic tube. A restrainer was inserted to limit the mobility of the mouse. The plastic tube was inserted into the Minispec LF50, and the program was executed. Any faeces or urine in the tube was cleaned away before the introduction of a new mouse.

3.10 Accuracy of Bruker's TD-NMR instrument

Before the experiment, a Minispec LF50 7.5 Hz TD-NMR instrument was purchased from Bruker. The instrument uses the principles of NMR to measure fat tissue mass in live mice. During the main experiment, the fat mass was measured weekly in all animals. At times, the instrument gave some strange readings. For instance, some animals showed decreased fat mass from one week to another, despite increasing body weight. Thus, we conducted a sub-experiment to investigate the correlation strength between the NMR measurements and large fat depots in the mice.

The fat tissue mass of 5 male and 5 female C57BL/6J Rj mice was measured using the Minispec LF50 from Bruker. The mice were then weighed before they were terminated by cervical dislocation. Subsequently, the abdomen of the mice was opened, and the large fat depots (epididymal/gonadal and visceral fat) were dissected and weighed. The intestine was stretched out to collect large patches of visceral fat; however, the dissection was relatively crude. One animal was excluded from the analysis as it had very large uteri filled with liquid, which would have impacted the weight measurement.

3.11 Sample power

The number of animals per experimental group was decided based on a Power analysis. The analysis was based on values from a study conducted by Alomaim and colleagues (Alomaim et al., 2019). They investigated the effect of Ca levels in rats fed a HF diet. In the Power analysis, we compared the means of the lowest Ca group to that of the highest Ca group. We ran a separate analysis on four variables, digestibility of 16:0 and 18:0, serum LDL levels, and total cholesterol.

Comparing C16:0 digestibility from the low-Ca group to the high-Ca group in the Alomaim study, a 20% difference between the two means would require a sample size of 2 ($\alpha = 0.05$, $\beta = 0.2$, $\sigma = 6$).

Comparing C18:0 digestibility from the low-Ca group to the high-Ca group, a 32% difference between the two means would require a sample size of 2 ($\alpha = 0.05$, $\beta = 0.2$, $\sigma = 8$).

Comparing serum total cholesterol from the low-Ca group to the high-Ca group, a 0,38 mmol/L difference between the two means would require a sample size of 12 ($\alpha = 0.05$, $\beta = 0.2$, $\sigma = 0.33$).

Comparing serum LDL cholesterol from the low-Ca group to the high-Ca group, a 0,10 mmol/L difference between the two means would require a sample size of 8 ($\alpha = 0.05$, $\beta = 0.2$, $\sigma = 0.07$).

Based on the Power analysis, we choose 10 animals per experimental group to be sufficient while still being statistically sound.

3.12 Statistics

Statistical analysis was performed using the software GraphPad Prism 9.2.0. For each analysis, considerations were made as to what statistical model was best suited to the data. Comparisons were considered significant if $p < 0.05$. When something is statistically significant, the result is not likely to occur by random chance; more likely, the result could be attributed to a specific cause. In this master thesis, a trend is defined by $p < 0.15$. For each analysis, the statistical model or test used is listed in the figure- or table text of the results. Normal distribution was checked with D'Agostino and Pearson normality tests.

3.13 Own contribution

In the last year, I have gained valuable experience in planning and executing animal experiments. I was included in the planning process from the start and had a say in how the experiment was set up (e.g., what to feed the mice, mice per group). Furthermore, another master student and I designed the diets (not chow) and calculated how much of each ingredient to add. We also ordered the ingredients and made the feed. The casein was separated from milk at the Dairy pilot at NMBU by the engineers working there. I performed the dry matter and Ca analyses of the casein.

I took part in writing the FOTS application; however, my supervisor Professor Harald Carlsen wrote most of it. Additionally, I took part in several meetings where the aim was to decide how to extract fat from faeces and analyse it. I reviewed the literature and suggested the Folch method, which was ultimately chosen.

In February, the animal experiment was initiated. Every weekday, I was present in the animal lab to check the welfare of the mice and measure weight, fat, and food consumption (Except one week where another master student and I came every other day due to Covid restrictions). Furthermore, I was at the animal lab 2 out of 5 weekends during the experiment to check their welfare and collect faeces. Additionally, I was part of the crew that terminated the mice, with my primary responsibilities being glucose measurements, injection of anaesthesia, blood sampling by cardiac puncture and cervical dislocation.

Another master student and I performed all procedures and analyses connected to the fat analysis in feed and faeces. Furthermore, we also analysed the chromatograms and calculated the amount of fat present in the samples.

My supervisor and I performed the sub-experiment where the objective was to assess the accuracy of the fat measurements by the Minispec LF50 from Bruker. I performed dissections on two mice.

I did not do any of the gene expression analyses as this was done by PhD student Dimitris Papoutsis. This was due to the Covid lockdown and the subsequent shutdown of the NMBU laboratories during the spring of 2021.

4 RESULTS

4.1 Effect of calcium on fatty acid digestibility and weight development in mice

4.1.1 Fatty acid digestibility as a function of calcium in the diet

Ca can form complexes with long-chain SFAs in the duodenum. We hypothesised that increasing amounts of Ca would affect FA uptake in the mice due to the excretion of insoluble CS in the faeces. During week 4 of the experiment, faeces were collected for all seven days, and food consumption was measured. Subsequently, the FAs were extracted and quantified from the feed and faeces. Thus, we calculated how much fat was consumed and how much fat the mice excreted over a 1-week period. These numbers were used to calculate % digestibility = (FA consumed - FA excreted) * (FA consumed)$^{-1}$ *100 for the FAs most abundant in faeces.

Table 4.1: % digestibility of four fatty acids (FA) in the mice fed a high-fat diet

	Groups				
	low-Ca	*mid-Ca*		*high-Ca*	
	But2	Che7	But7	Che20	But20
14:0	99.7 ± 0.1^{a}	99.3 ± 0.2^{ab}	99.4 ± 0.2^{ab}	98.8 ± 0.7^{b}	98.9 ± 0.2^{b}
16:0	99.1 ± 0.5^{a}	97.8 ± 0.5^{ab}	97.9 ± 0.6^{ab}	96.4 ± 1.7^{b}	96.5 ± 0.7^{b}
18:0	97.8 ± 1.4^{a}	95.3 ± 1.0^{ab}	95.2 ± 1.1^{ab}	92.0 ± 3.5^{b}	91.8 ±1.8^{b}
18:1*cis9*	99.9 ± 0.1^{a}	99.8 ± 0.1^{ab}	99.8 ± 0.04^{ab}	99.6 ± 0.2^{bc}	99.5 ± 0.2^{c}

Food consumption and faeces were measured over the duration of a week (week 4). FA content of the feed and faeces were quantified using chemical analysis and GS. % digestibility = (FA consumed – FA faeces) * (FA consumed)$^{-1}$ * 100 was calculated for week 4 of the experiment. Differences among means were analysed using a one-way ANOVA with Tukey's multiple comparison test performed using GraphPad Prism version 9.2.0 (Graphpad Software, USA). Groups marked with identical letters indicate no significant difference, whereas groups marked with different letters indicate significant difference. Abbreviations: FA = Fatty acid, GS = Gas Chromatography, Ca = Calcium, ANOVA = Analysis of variance

Table 4.1 shows an overview of the four most abundant FAs in the faeces of mice fed an HF diet. All other FAs present in the faeces were below the cut-off point, meaning that their % digestibility was between 99 and 100. The % digestibility for 14:0 was very high for all HF groups. While minor, a reduction of 1% digestibility was still observed in the high-Ca groups compared to the low-Ca group for 14:0. Moreover, the % digestibility of 16:0 is reduced by approximately 2.5% in the high-Ca groups compared to the low-Ca group (from ~99% to 96.5%). The most considerable impact of Ca was seen on 18:0 % digestibility. A significant reduction of about 6% was observed in the high-Ca groups compared to the low-Ca group.

Additionally, there was a trend that all high-Ca groups experience reduced 18:0 % digestibility compared to the mid-Ca groups (P-values=0.12); however, these observations were not significant. The only unsaturated FA that made it above the cut-off point, 18:1*cis*9, revealed a significant yet very slight reduction in % digestibility with increasing Ca levels. A 0.4% reduction was observed in high-Ca groups compared to the low-Ca group.

The evidence suggests that Ca is only able to make complexes with FFAs. NLs (e.g., TAG, DAG, MAG) should generally not be affected by varying Ca levels in the feed. Fat found in the faeces was separated into FFAs and NLs by SPE to investigate whether this was the case. Table 4.2 shows the contribution of the FFA and NL fractions to the total amount of 16:0 discovered in the faeces of the butter groups, given in percent. Generally, the FFAs contributed between 90 and 95% to the 16:0 content of the faeces, while NLs contributed between 5 and 10%. A higher contribution of FFAs to the 16:0 content of the faeces was seen in the high-Ca group compared to the low-Ca group.

Table 4.2: contribution of the free fatty acid (FFA) fraction and neutral lipids (NL fraction to the total amount of Palmitic acid (16:0) found in the faeces of high-fat butter groups, given in percent

But2		**But7**		**But20**	
NL	FFA	NL	FFA	NL	FFA
9.06 %	90.94 %	8.21 %	91.79 %	5.75 %	94.25 %
8.31 %	91.69 %	8.84 %	91.16 %	8.51 %	91.49 %
4.17 %	95.83 %	8.02 %	91.98 %	4.49 %	95.51 %
6.25 %	93.75 %	4.25 %	95.75 %	4.21 %	95.79 %
8.90 %	91.10 %	6.46 %	93.54 %	5.30 %	94.70 %

Total fat was extracted from faeces and was subsequently divided into FFA and NL fractions by solid phase extraction. The two fractions were quantified by gas chromatography and mass spectrometry to determine the amount present in faeces. The results in the table were calculated by dividing the fraction (FFA or NL) on the total fat content extracted from the faeces.

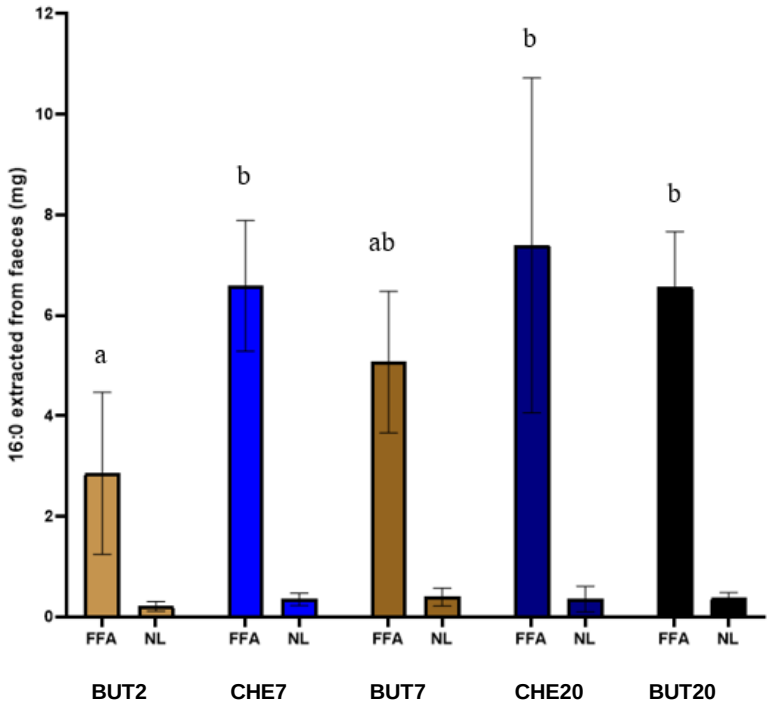

Figure 4.1: The total amount of free fatty acids (FFA) and neutral lipids (NL) of Palmatic acid (16:0) found in the faeces of all HF diet groups. Differences among the means of the FFA fraction were analysed using a one-way ANOVA with Tukey's multiple comparison test, performed using GraphPad Prism version 9.2.0 (Graphpad Software, USA). Groups marked with identical letters indicate no significant difference, whereas groups marked with different letters indicate significant difference. Variance is shown as standard deviation. Abbreviations: ANOVA = Analysis of variance

Moreover, Figure 4.1 shows the total amount of FFAs and NLs of 16:0 found in the faeces of HF-diet groups. No significant differences were found between the groups with regards to the NL fractions. However, a one-way ANOVA revealed significantly more FFAs in the high-Ca groups (Che20 P-value=0.0106 and But20 P-value=0.0462), and one of the mid-Ca groups (Che7 P-value=0.0438) compared to the low-Ca group.

Our results show that Ca impacted FA digestibility in mice receiving HF diets, in a dose dependent manner. Mice on a high-Ca/HF diet had 2.5% lower uptake of 16:0 and 6% lower uptake 18:0 compared to mice fed a low-Ca/HF-based diet. Furthermore, there was 10-20 times more FFAs of Palmitic acid in the faeces compared to NLs. Ca significantly impacted the amount of 16:0 FFA found in the faeces of the high-Ca groups and the mid-Ca cheese group compared to the low-Ca group.

4.1.2 Effect of calcium on weight development

To evaluate whether Ca affected weight development in the mice, they were weighed once a week for the duration of the experiment. Food consumption was also measured weekly to calculate energy intake during the feeding period.

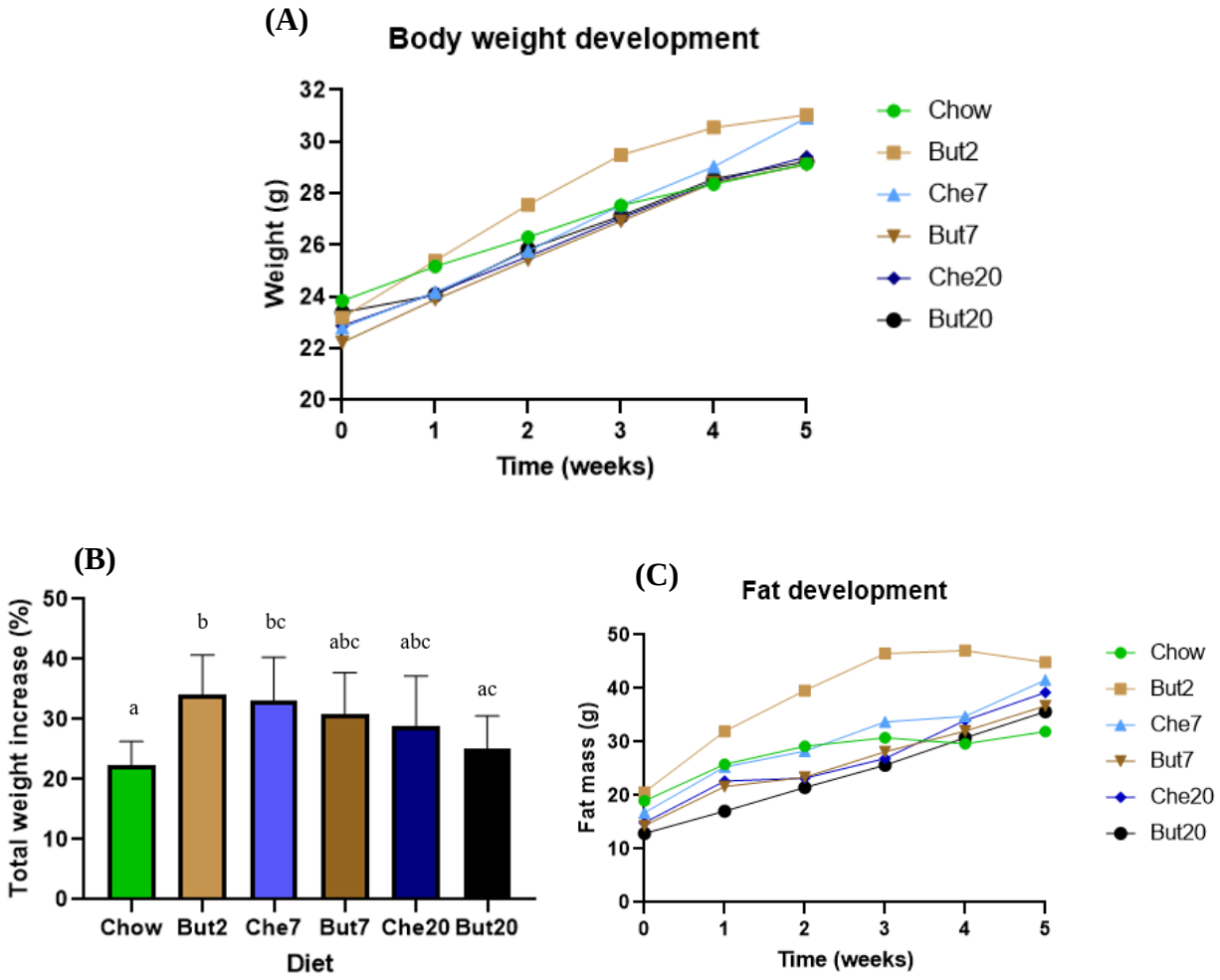

Figure 4.2: Body weight development in groups of mice fed different diets. (A) shows the weekly change (%) in body weight of the groups until the week of termination. Week 0 represents the baseline weight of the animals. **(B)** Shows the total weight increase of the animals given in percent adjusted for baseline weight differences. Differences among means were analysed using a one-way ANOVA with Tukey's multiple comparison test. Groups marked with identical letters indicate no significant difference, whereas groups marked with different letters indicate significant difference. **(C)** is an overview of body fat development in the mice. Fat mass was measured by a body composition analyser (Minispec LF50, Bruker). Variance is shown as standard deviation. The graphs with corresponding statistical tests were performed using GraphPad Prism version 9.2.0 (Graphpad Software, USA). Abbreviations: ANOVA = Analysis of variance

As shown in Figure 4.2.A, mice weight at baseline was not identical despite being randomly distributed into the different experimental groups. After 1 week of feeding high fat fed groups started to separate clearly in weight. But2 mice weighed the most and continued to do so until termination. The Chow animals weighed the most at baseline but had the lowest body weight at the end of the experiment. While the weight gain stagnated for most groups the last week of the feeding trial, the Che7 group increased their weight gain the last week, almost overtaking the But2 group in total body weight.

Figure 4.2.B shows that the Chow group gained the least amount of weight. While all the other groups gained more weight than the Chow group, the association was only significant for But2 (P-value=0.0028) and Che7 (P-value=0.0075). Furthermore, an increase in dietary Ca levels may be associated with less body weight. However, But20 was the only group where weight gain was significantly (P-value=0.0421) decreased compared to the low-Ca group.

Fat tissue mass was measured weekly by a TD-NMR instrument (Figure 4.2.C). The But2 group produced the highest fat readings for the duration of the experiment. The other groups exhibited similar fat development, except the Chow mice, with fat gain decelerating the last couple of weeks. However, the instrument produced peculiar readings (e.g., fat tissue mass decreasing, despite body weight increasing) during the experiment's later stages due to desyncing between the software and electronics. Thus, there was large variations in the data of weeks 4 and 5.

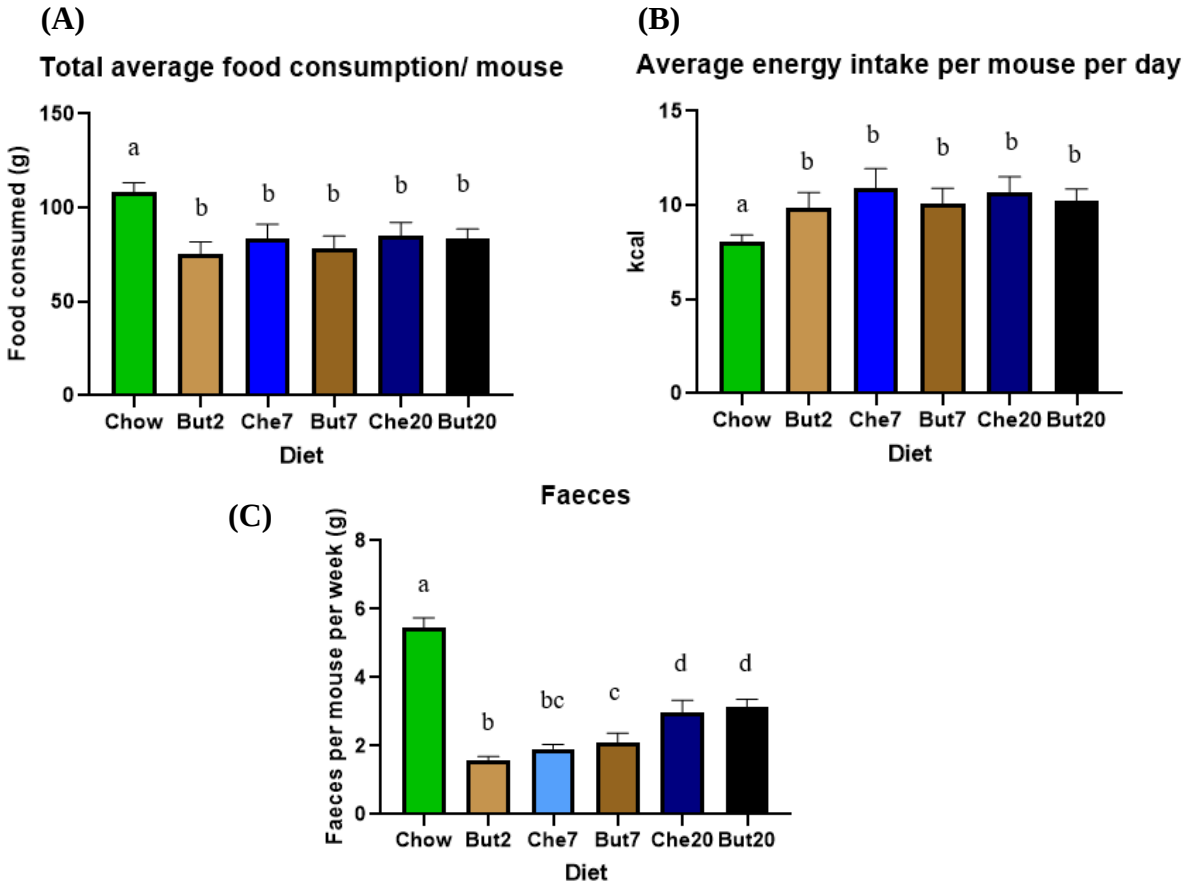

Figure 4.3: Total food consumption, average energy intake and faeces excreted. (A) Shows the total average amount of food consumed per mouse. **(B**) Shows the total average energy intake per mouse for groups fed different diets. Calories consumed was calculated for every week and added together to demonstrate the total caloric intake of the mice. **(C)** Shows the amount of faeces (g) excreted per mice over the period of one week. Differences among means were analysed using a one-way ANOVA with Tukey's multiple comparison test, performed using GraphPad Prism version 9.2.0 (Graphpad Software, USA). Groups marked with identical letters indicate no significant difference, whereas groups marked with different letters indicate significant difference. Variance is shown as standard deviation. Abbreviations: kcal = Kilo calories, ANOVA = Analysis of variance

As seen in Figure 4.3.A, the Chow mice consumed more food than the other groups. Between the HF groups, there were no significant differences in food consumption.

Figure 4.3.B illustrates the average energy intake per mouse per day of all the groups. While the chow mice ate more mass than the HF mice, their feed contained less energy. Hence, the Chow group total energy intake was significantly lower than all other groups. Among the HF groups, there were no significant differences in daily average energy intake.

To investigate whether the different diets affected faecal excretion differently, faecal mass was weighed over a seven-day period and displayed as gram faeces per mouse per week (Figure 4.3.C). As expected, chow mice produced significantly more faeces than the HF diet groups because they ate more food and the food was also rich fermentable dietary fibres. Interestingly, the high-Ca groups produced significantly more faeces than the mid -and low-Ca groups. Furthermore, the But7 group excreted significantly (P-value=0.0453) more faeces than the But2 group.

The food and energy consumption between the HF diet groups were approximately the same. Additionally, there was a pattern emerging where increasing Ca in the feed was associated with an increasing amount of faeces excreted.

We further observed that mice in the high-Ca groups, excreted faeces with visible blood content. Occasionally, blood was also observed in the faeces of mid-Ca; however, it was much more frequent in the high-Ca groups. No blood was observed in the But-2 or Chow groups.

In summary, Ca content affected weight gain in the mice that received HF butter-based diets with a lower weight gain (-9%) in the high-Ca group compared to the low-Ca group. The effect of Ca on weight gain was not found in the mice that received the cheese-based HF diet. No effect of Ca was found on body fat mass development. The daily average energy intake per mouse was approximately equal for all HF groups. Furthermore, Ca had a dose dependent effect on faeces excretion, where the High-Ca excreted the most. Blood content was observed in the faeces of high-Ca mice.

4.2 Influence of matrix on fatty acid digestion and weight development

The main hypothesis for a potentially health neutral outcome of SFA rich cheese intake, is its high content of Ca creating CSs with long chain SFAs. However, other mechanisms have been proposed as possible explanations. Hence, we investigated whether any effect in FA digestibility and inflammation could be attributed to something other than Ca in the cheese (a so-called matrix effect). Matrix effects were investigated by comparing butter and cheese feeds that were very similar in both FA content and composition. As no low-Ca cheese group was included in the design, the low-Ca butter group was excluded from the matrix analysis.

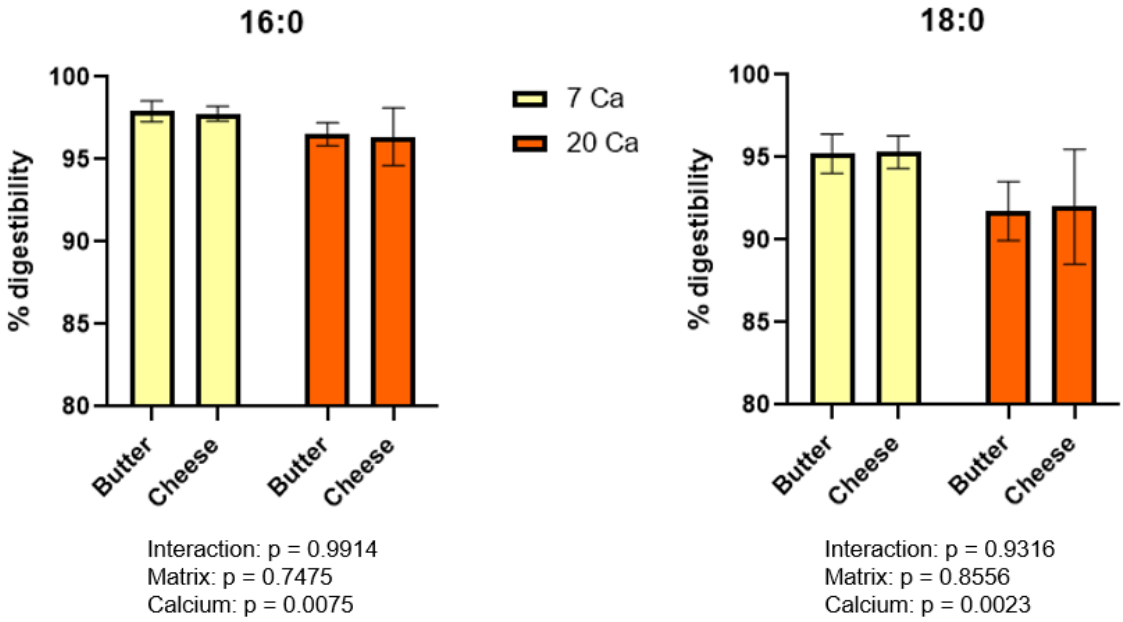

Figure 4.4: Effect of matrix on 16:0 and 18:0 % digestibility. A two-way ANOVA with Tukey's multiple comparison test was performed with the two variables matrix and Ca, using GraphPad Prism version 9.2.0 (Graphpad Software, USA). The groups included in the analysis were the mid-Ca and high-Ca groups: Che7, But7, Che20 and But20. P-values are shown for the interaction term, and main effects matrix and Ca. **NB**, the y-axis starts at 80% and not 0. Variance is shown as standard deviation. Abbreviations: 16:0 = Palmitic acid, 18:0 = Stearic acid, Ca = Calcium, ANOVA = Analysis of variance

A two-way ANOVA revealed no effect of the matrix on 16:0 and 18:0 % digestibility (Figure 4.4). Moreover, no interaction between the two main effects, Ca and matrix, were observed. However, Ca impacted the two FAs significantly in both groups, with a reduction in digestibility observed in the high-Ca groups.

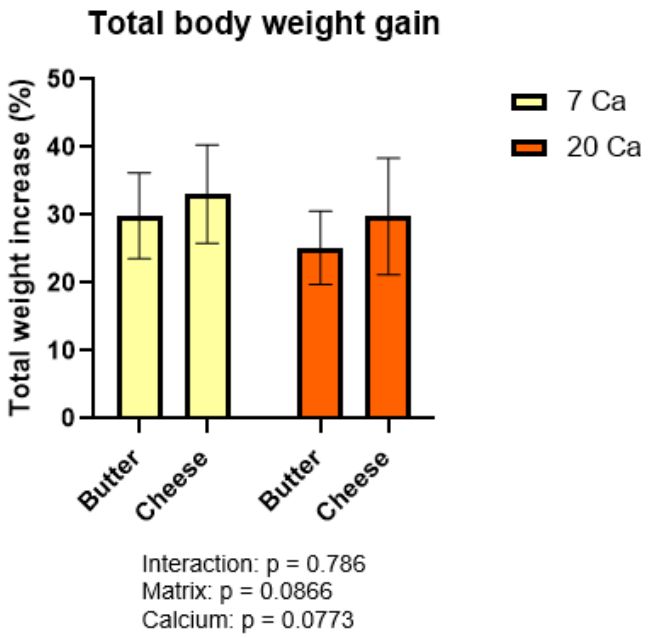

Figure 4.5: Effect of matrix on the total body weight. A two-way ANOVA with Tukey's multiple comparison test was performed with the two variables matrix and Ca, using GraphPad Prism version 9.2.0 (Graphpad Software, USA). The groups included in the analysis were Che7, But7, Che20 and But20. The figure shows the effect of matrix on total body weight gain. The p-values of the interaction term and the two main effects, matrix and Ca, are shown. Variance is shown as standard deviation. Abbreviations: Ca = Calcium, ANOVA = Analysis of variance

Figure 4.5 revealed a trend that matrix (p-value=0.0866) and Ca (p-value=0.0773) influenced total weight gain of the mid- and high-Ca mice. The mice fed a butter diet seemed to have gained slightly less weight than mice fed a cheese diet. Moreover, the mice fed a high-Ca diet may have gained slightly less weight than mice fed a mid-Ca diet.

In summary, a matrix effect was not observed with regards to 16:0 and 18:0 digestibility. However, there was a trend that the matrix influenced the total weight gain of the mice (p-value=0.0866).

4.3 Expression of genes related to intestinal health

Certain long-chain SFAs, like 14:0 and 16:0, have been shown to induce inflammation in the small intestine. We hypothesised that Ca would bind long-chain SFAs and were interested to check whether this would influence intestinal health. The expression of four relevant genes was examined to evaluate intestinal health. TNF-α is an inflammatory cytokine that has been consistently shown to be upregulated during inflammation in the small intestine. iNOS encodes inducible nitric oxide synthase and is highly responsive to inflammatory stimuli whereas NOX2 encodes NADPH oxidase type 2, which is crucial for initiating oxidative burst in innate immune cells. Elevated levels of iNOS and NOX2 mRNA is therefore a good indication of inflammation and putative increase in reactive oxygen- and nitrogen species

(ROS/RNS). ROS/RNS are, among various other mechanisms, generated as a cellular response to pathogens (Morgan & Liu, 2011; Quinn et al., 2006). *ZO-1* is a tight junction gene. It encodes a protein whose purpose is to keep the epithelial cells of the barrier tight together. A low expression of the gene is often associated with decreased barrier function by the mechanism of increased paracellular permeability (Murakami et al., 2016).

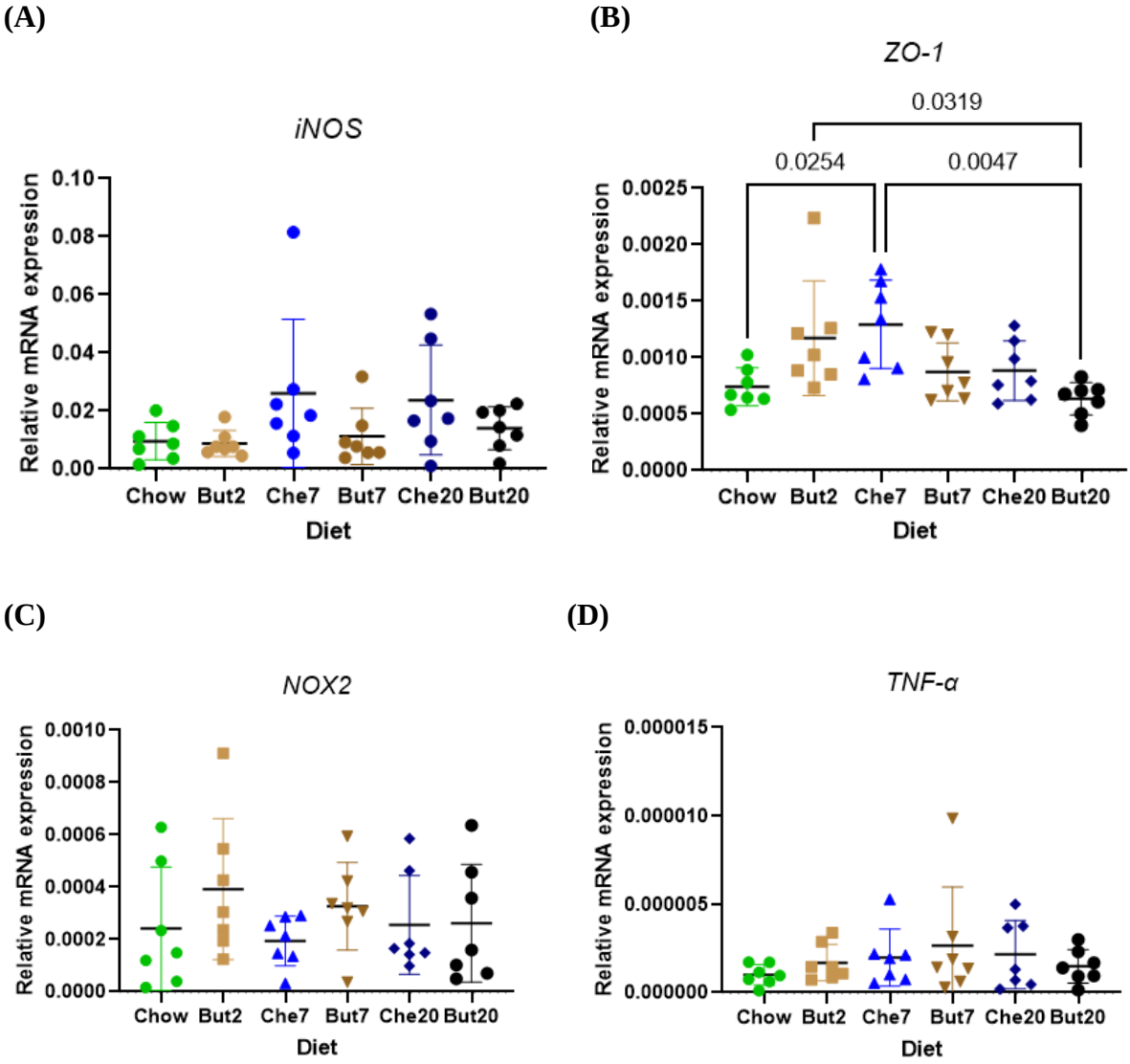

Figure 4.6: Relative mRNA expression of genes related to intestinal health. mRNA gene expression of **(A)** *iNOS*, **(B)** *ZO-1*, **(C)** *NOX2* and **(D)** *TNF-α* relative to the basal expression of the housekeeping gene *GAPDH*. Variation within groups is given as SEM (n=7). Differences among means were analysed using a one-way ANOVA with Tukey's multiple comparison test, using GraphPad Prism version 9.2.0 (Graphpad Software, USA). Significant differences between groups are shown with p-values and no p-value means no significant difference. Abbreviations: mRNA = Messenger ribonucleic acid, iNOS = Nitric oxide synthase, ZO-1 = Zonula occludens 1, NOX2 = NADPH oxidase 2, TNF-α = Tumour necrosis factor α, GADPH = Glyceraldehyde 3-phosphate dehydrogenase, ANOVA = Analysis of variance, SEM = Standard error of the mean

Figure 4.6 A, C and D illustrate the relative mRNA expression of *iNOS*, *NOX2* and *TNF-α*. Different HF diets did not produce any significant difference in the expression of the genes mentioned above. Furthermore, *iNOS*, *NOX2* and *TNF-α* expression was not significantly different between the Chow and HF diet groups. However, some differences in the expression of *ZO-1* between the groups were evident. *ZO-1* mRNA expression was lowest in the But20 group, and this observation was significant compared to But2 (P-value=0.0319) and Che7 (P-value=0.0047). Additionally, the Che7 group had a higher expression of the gene than the Chow group (P-value=0.0254). To further analyse *ZO-1* expression with respect to matrix effects, a two-way ANOVA test was conducted (Figure 4.7). Interestingly increased *ZO-1* expression was dependent on matrix (P-value=0.0040) and Ca (P-value=0.0049). As shown in Figure 4.7, the gene was upregulated in the cheese groups in comparison to the butter groups and reduced by increasing amounts of Ca. No significant interaction effect between the two main effects, Ca and matrix, was observed.

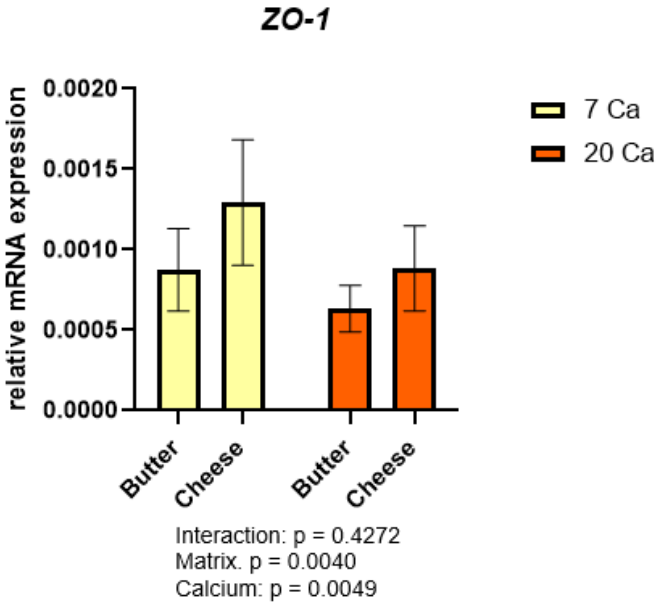

Figure 4.7: Effect of matrix on expression of the tight junction gene *ZO-1*. A two-way ANOVA with Tukey's multiple comparison test was performed with the two variables matrix and Ca, using GraphPad Prism version 9.2.0 (Graphpad Software, USA). The groups included in the analysis were Che7, But7, Che20 and But20. The figure shows the effect of matrix on relative gene expression of *ZO-1*. The p-values of the interaction term and the two main effects, matrix and Ca, are shown. Abbreviations: Ca = Calcium. ZO-1 = Zonula occludens 1, ANOVA = Analysis of variance

Overall, no effects of Ca were seen on the expression of inflammation markers in the small intestine. However, the tight junction gene *ZO-1* had the highest expression when HF diets were added low Ca levels (for butter-based HF diet) and medium Ca levels (for cheese-based HF diet). Furthermore, a significant effect of the matrix was found on the expression of *ZO-1*, with the gene being higher expressed in cheese-based diets compared to butter-based diets.

4.4 Accuracy of Bruker's Minispec LF50 on fat mass measurements

A TD-NMR (Minispec LF50 7.5 Hz, Bruker) instrument was used to measure fat mass in the mice during the main experiment. The device was recently purchased and had thus not been used in experiments before. The instrument worked well for the first 3 weeks of the experiment; however, it produced some unexplainable measurements during the last two weeks (e.g., the fat mass had decreased compared to previous weeks while body weight increased). Thus, the accuracy of the Bruker TD-NMR instrument was evaluated by dissecting out major fat depots (gonadal/epididymal, visceral fat) from mice and comparing them to the measurements given by the instrument in the same mice (Table 4.3). Additionally, mice were weighed to investigate whether dissected fat or NMR measurements were good predictors of body weight.

Table 4.3: Weight of mice, fat mass values given by TD-NMR and weight of large fat depots dissected out

Mouse ID	Sex	Weight (g)	Fat TD-NMR (g)	Fat dissected (g)
711-1	F	23.62	3.587	0.58
711-3	F	23.16	1.707	0.27
711-4	F	27.00	6.284	1.58
711-5	F	25.06	3.722	0.63
708-1	M	32.87	2.896	0.70
708-2	M	32.75	4.960	1.51
708-3	M	32.75	5.424	1.02
708-4	M	38.95	9.838	2.58
708-5	M	36.90	8.201	2.37

Mouse 711-2 was excluded from the dataset as it had abnormally large uteri. Abbreviations: ID = Identification, TD-NMR = Time-domain nuclear magnetic resonance.

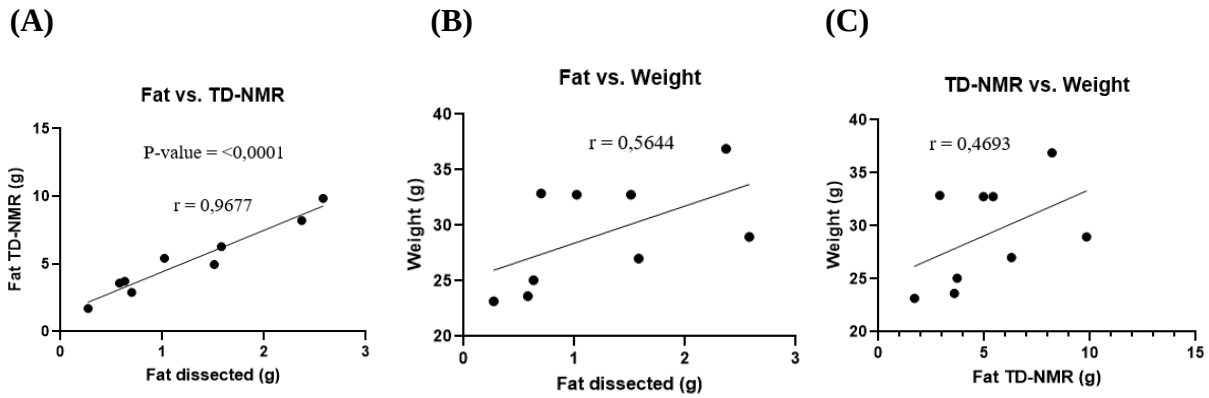

Figure 4.8: Correlation between the three variables fat, TD-NMR and weight. (A) shows the correlation between fat dissected out and fat measurements given by the TD-NMR instrument. **(B)** shows the correlation between dissected fat and body weight, while **(C)** shows the correlation between TD-NMR measurements and body weight. Analysis of correlation was performed using Spearman's Rho (given as the r-value) to investigate the strength of association between the variables, using GraphPad Prism version 9.2.0 (Graphpad Software, USA). Abbreviations: TD-NMR = time-domain nuclear magnetic resonance

Figure 4.8 A shows a simple linear regression plot describing the association between fat tissue mass measurements given by the TD-NMR instrument and fat dissected out of the mice. The amount of fat dissected was highly correlated to the measurements given by the instrument, with an R-value equal to 0.9677 (Spearman's Rho). Interestingly, neither fat dissected, nor TD-NMR measurements were highly correlated to the weight of the mice with Spearman’s Rho of 0.5644 and 0.4693 (Figure 4.8 A and 4.8 B).

5 DISCUSSION

High intake of SFAs has consistently been shown to raise low-density lipoprotein cholesterol, a known risk factor of CVD. One of the most significant single contributors of SFAs to the diet is cheese. While containing high amounts of SFAs, cheese itself does not seem to increase the risk of disease. The high Ca content in cheese has been proposed to explain this paradox through limiting the uptake of long-chain SFAs by forming insoluble soaps. Also, other abilities of the cheese have been suggested to affect SFA uptake through a so-called matrix effect.

Several rodent studies have shown that increasing Ca levels in the diet leads to increasing amounts of SFAs in the faeces. Furthermore, a lesser uptake of SFAs like 16:0 and 18:0 could have implications for the individual's overall health status. Ca has been proposed to be associated with less weight gain, lower cholesterol, and less fat in the liver. Thus, a better understanding of fat and Ca and how they affect markers of disease is desirable.

The purpose of this project was to investigate whether Ca impacts the long-chain FA digestibility and weight development in mice. Furthermore, we wanted to investigate whether Ca or matrix could affect the expression of genes related to intestinal health.

In this study, it was demonstrated that Ca affected long-chain SFA digestibility and weight development in mice. Additionally, Ca impacted barrier function; however, no effects were observed on inflammatory markers. While no effect of the fat matrix was seen on FA digestibility and inflammation, it did impact weight development and the expression of the tight junction gene, *ZO-1*. Furthermore, the Minispec LF50 from Bruker was a reliable predictor of fat tissue mass in the mice.

5.1 Calcium affects fatty acid digestibility and weight development

5.1.1 Effect of calcium on fatty acid digestibility

The interplay between Ca and fat is not fully understood, yet it could play a protective role in the onset of diet-induced diseases. First and foremost, we wanted to investigate to what extent Ca affected the digestibility of individual FAs. Food consumption and faeces excretion were measured in the mice for one week (week 4 of the experiment). Subsequently, the FAs were quantified in the feed and faeces by use of a GC-MS. After that, % digestibility was calculated by comparing the FAs consumed to FAs excreted.

Overall, we found the effect of Ca on FA digestibility to be less than expected. Digestibility of 18:0 was found to decline 6% in high-Ca groups compared to the low-Ca group. Furthermore, a decrease of only 2.5% was observed in 16:0 digestibility from low- to high-Ca groups. While significant, the marginal effect of Ca on 16:0 and 18:0 digestibility is surprising, as many have reported a much more substantial effect.

Alomaim and colleagues fed rats a HF diet with varying amounts of Ca and reported a 20% decrease in 16:0 and a 30% decrease in 18:0 digestibility in rats fed high amounts of Ca compared to rats fed low amounts of Ca (Alomaim et al., 2019). Indeed, several other rodent studies also show significantly more faecal fat in animals fed a high-Ca diet than a low-Ca diet (Ayala-Bribiesca et al., 2018; de Wit et al., 2011; Papakonstantinou et al., 2003).

The evidence on Ca and its effect on obesity and markers of disease is dividing. Still, most *in vivo* studies investigating Ca's effect on fat digestibility/excretion find an association between the two (Alomaim et al., 2019; Davies et al., 2000; de Wit et al., 2011; Papakonstantinou et al., 2003). Furthermore, CS formation and precipitation have been studied in several *in vitro* systems (Devraj et al., 2013; Graham & Sackman, 1983; Pereira et al., 2012), leaving no doubt that Ca possess the ability to make insoluble complexes with FAs. However, while Ca complexation with FAs occurs, there is no guarantee that precipitation will happen (which is necessary if the complex is to be excreted in the faeces). Whether the complex stays in solution or precipitates likely depends on just the right balance between hydrophobic factors and the water present in the system (Pereira et al., 2012). It may be that the mouse intestine, in conjunction with the diet consumed, did not provide the optimal system for CS precipitation in our experiment. Most studies on the effect of Ca on FA digestibility are rat studies (Alomaim et al., 2019; Ayala-Bribiesca et al., 2018; Papakonstantinou et al., 2003). However, de Wit et al. investigated the effect of Ca on fat excretion in C57BL/6J mice fed an HF diet (de Wit et al., 2011). They observed 2.4 times more faecal fat in mice fed a high-Ca HF diet compared to a low-Ca HF diet. Nevertheless, it is worth noting that they did not look at individual FAs like we did, which makes it difficult to compare their results to ours directly.

While a significant effect was observed between high-Ca and low-Ca groups in digestibility of 14:0 and 18:1cis9, it was only marginal. 14:0 digestibility decreased by approximately 1%, while 18:1cis9 digestibility decreased by only 0.4%. Digestibility of these FAs is affected less than 16:0 and 18:0, a pattern supported in the literature (Alomaim et al., 2019; Ayala-Bribiesca et al., 2018; de Wit et al., 2011; Papakonstantinou et al., 2003). While Ca can interact with many FFAs, the solubility of the resulting CS will vary. An experiment by Graham and Sackman showed that the solubility of the CS was inversely correlated with pH, carbon-chain length, and degree of FA saturation (Graham & Sackman, 1983). In line with these observations, our results demonstrating that 18:0 was less digested by high-Ca (6% reduction) than 16:0 (2.5% reduction), 14:0 (1% reduction) and 18:1cis9 (0.5% reduction) makes sense. 14:0 does not have a long enough hydrocarbon chain, and 18:1*cis9* does not contain the degree of saturation required to form CS insoluble enough to affect digestion substantially. Furthermore, other FAs found in the faecal samples did not provide a signal exceeding the cut-off point, which implies a very efficient uptake of these FAs.

We observed visible blood content in the faeces of mice fed high-Ca diets. Bloody faeces may be a symptom of GI-related diseases. However, the mice seemed healthy overall, and gene expression analysis did not reveal any difference in inflammatory status between the high-Ca and the low-fat Chow control group. A possible explanation could be that a high faecal fat content increased the stool hardness in the high-Ca groups, damaging their GI tracts. This phenomenon is described in infants fed milk formulas instead of human milk (Quinlan et al., 1995). Human milk contains 53-57% of the 16:0 in the *sn2*-position, which means that the uptake of 16:0 in breastfed infants will be excellent. In contrast, early milk formulas contained most 16:0 at the *sn1*- and *sn3*-positions. Pancreatic lipase cleaves the FAs connected to the *sn1* and *sn3*-positions, leaving the subsequent FFAs free to interact with Ca and form soaps. Quinlan and colleagues found faecal 16:0 content to be very high in infants fed milk formulas. Furthermore, faecal excretion of CSs was correlated with stool hardness, which may explain the visible blood content we observed in the faeces of high-Ca mice.

In summary, our results show that Ca impacts FA digestibility in mice receiving HF diets, in a dose dependent manner. Mice on a high-Ca/HF diet had 2.5% lower uptake of 16:0 and 6% lower uptake of 18:0 compared to mice fed a low-Ca/HF-based diet. A slight reduction in 14:0 and 18:1*cis9* digestibility was also observed. However, the effect of Ca on FA digestibility was not as large as expected.

5.1.2 Effects of calcium on weight development

Obesity has reached epidemic proportions. Fat is the most calorie-dense of the macronutrients and is thus of great interest to both the food and health sector. We wished to investigate the effect of Ca on weight development, as this could add to the knowledge of nutrition and obesity.

This study revealed that Ca content affected weight gain in the mice that received HF butter-based diets. Mice fed low-Ca butter diet gained 9% more weight than those fed a high-Ca butter diet over five weeks. The evidence on the effect of Ca on weight development is conflicting. Some rodent studies (Alomaim et al., 2019; de Wit et al., 2011) and human studies (Haub et al., 2005; Reid et al., 2005; Shapses et al., 2004) observed no beneficial effects of Ca on weight development. On the other hand, Papakonstantino and colleagues reported similar results reported in this study as they found control rats to gain 335 g of weight, while rats fed a high Ca diet gained 310 g of weight (Papakonstantinou et al., 2003). Additionally, Davis and co-workers reviewed a randomised controlled trial in humans where the Ca-supplemented group lost 0.671kg per year, and the placebo-control group lost 0.325 kg body weight per year, over a 4-year period (Davies et al., 2000).

Davies and Papakonstantino argue that the weight reduction is explained by increased CS formation with FAs in the high-Ca groups, leading to decreased energy intake in these groups. We observed a decrease of 6% in 18:0 digestibility and a 2.5% decrease in 16:0 digestibility (Davies et al., 2000; Papakonstantinou

et al., 2003). Ultimately, the reduced absorption of the two FAs only accounts for a decrease in total energy intake of <0.5% in the But20 group compared to the But2 group. Such a minor decrease in energy intake is not enough to explain a 9% weight gain difference between the groups. Thus, the observed weight gain difference is most likely not due to the formation of insoluble CSs. Moreover, a difference in ingested energy could potentially explain the weight difference. However, as seen in Figure 4.3.B, the HF groups ingested approximately the same amount of energy.

Interestingly, the mice fed a high-Ca diet produced twice as much faeces as those fed a low-Ca diet (Figure 4.3.C). As previously determined, the high-Ca groups excrete more FAs than the low-Ca group. While the high-Ca groups excrete slightly more FAs than the low-Ca group, it is not enough to explain the 2-fold increase in faeces produced. A possible explanation could be that Ca precipitate bile acids, which are subsequently excreted in the faeces. Ca predominantly makes complexes with the secondary conjugated hydrophobic bile acids, such as deoxycholic acid (DCA) and lithocholic acid (LCA) (Govers et al., 1996). Alomaim and co-workers reported a 3-fold increase and a 4-fold increase of DCA and LCA in the faeces of high-Ca rats compared to low-Ca rats (Alomaim et al., 2019). Increased bile excretion due to interactions with Ca could explain why high-Ca mice produce more faeces than the others. Furthermore, the production of large quantities of faeces is an energy-demanding process. Additionally, bile acids lost in the faeces means that the *de novo* synthesis of bile needs to be upregulated, which also requires energy. Consequently, the metabolic activity in these mice might be higher. This may be part of the explanation as to why high-Ca mice gained less weight than low-Ca mice.

In summary, we found the low-Ca group to have gained significantly more weight than the high-Ca group, But20, over five weeks. The difference in weight gain is most likely not explained by faecal fat excretion but may be explained by increased metabolic activity in the high-Ca mice.

5.2 Matrix effects

There is an increasing interest in the so-called matrix effect of foods. Foods might be similar in composition (nutrients and calories) yet have a distinctly different physiochemical structure that affects health differently. An effect of the matrix is not unheard of and has, e.g. been shown to influence satiety when carrots were given in different structures (whole carrots, blended carrots and carrot nutrients) (Moorhead et al., 2006). Dairy products share many similarities (especially FA composition) yet come in vastly different shapes and forms; butter and (most) cheeses are solid, yoghurt is semi-solid, and milk is liquid. A literature search reveals only a handful of articles that evaluate different dairy products and the effect of matrix on lipid digestion and metabolism, elucidating the need for further research on the topic.

A two-way ANOVA revealed no effect of matrix on 16:0 and 18:0 digestibility. Our results are similar to Soerensen et al., who investigated the effect of Ca in cheese versus Ca in milk in humans (Soerensen et

al., 2014). They observed a higher faecal lipid loss in the cheese and milk groups compared to the control; however, no differences in faecal fat were observed between the dairy product groups. The findings of Soerensen et al. underlines our sentiment that the Ca level in the feed is main influencer of faecal fat excretion.

Soerensen et al. compared cheese to milk, while we compared cheese to butter. Few others have done so; however, there are some: Hjerpsted et al. conducted a randomised cross-sectional study where they investigated the effects of daily consumption of a hard cheese compared with butter for 6 weeks (Hjerpsted et al., 2011). They found the cheese intervention to lower plasma- total cholesterol, LDL cholesterol and HDL cholesterol, compared to the butter intervention. Plasma LDL cholesterol was 6.9% lower in the cheese group. The Hjerpsted et al. results agree with an earlier study from Tholstrup et al. where subjects had 20% of their daily energy intake derived from either cheese or butter (Tholstrup et al., 2004). They observed that cheese consumption led to lower serum- total cholesterol and LDL cholesterol levels compared to butter consumption over time.

As seen in Figure 4.5, there is a trend (p-value=0.0866), though not significant, that matrix affected body weight development in our mice. Soerensen et al. argues that the Ca in cheese is in part bound to the casein, which may facilitate more interactions between fat and Ca in cheese than butter, as much of the fat is structured within the casein-Ca matrix (Soerensen et al., 2014). However, as neither Soerensen et al. nor we observed an effect of matrix on faecal fat excretion, it seems unlikely that increased Ca-fat interactions would make a noticeable impact.

Our findings and others (Clemente et al., 2003; Fruekilde & Høy, 2004; Hjerpsted et al., 2011; Tholstrup et al., 2004) suggest that the matrix effect of different dairy products could potentially impact health. However, the mechanisms are somewhat unclear. Drouin-Chartier et al., who observed a higher TAG response induced by cream cheese compared to cheddar, argued that this could result from differences in lipid droplet size (Drouin-Chartier et al., 2017). Lipid droplets from cream cheese will have a diameter of about 0.5 um, while cheddar cheese forms lipid droplets approximately six times bigger (3.0 µm). Smaller lipid droplets have an increased surface area that digestive enzymes can access, which is well known to be advantageous for lipolysis rates (Mu & Høy, 2004; Wang et al., 2013). Lipid droplets from cheddar will be larger than from cream cheese, as the fat globule of cheese will often be organised within the protein matrix (Drouin-Chartier et al., 2017).

In summary, no matrix effect was observed on 16:0 and 18:0 digestibility. However, there was a trend that matrix affected the weight development of the mice.

5.3 Inflammation and gut barrier integrity

We discovered no differences in gene expression of the inflammatory markers *TNF-α*, *iNOS* and *NOX2* between the HF groups. Furthermore, no difference in inflammatory levels was observed between the HF and the chow groups (low-fat). The similarities of the inflammatory levels of the chow and HF diet groups are surprising, as a HF diet is generally shown to induce inflammation in the small intestine (Ding et al., 2010; Wang, N. et al., 2013). A possible explanation could be the short length of the intervention. The mice were terminated after 5 weeks, which might not have given the HF diet mice enough time to develop intestinal inflammation. However, Wang et al. saw significant increases in the pro-inflammatory cytokines *TNF-α* and IL-6 in C57BL/6 mice after only 7 days of HF feeding (Wang, N. et al., 2013). Furthermore, Ding et al. observed a significant difference in ileal *TNF-α* expression between mice fed a low-fat and HF diet after 6 weeks (Ding et al., 2010).

The lack of results could reflect a poor choice of inflammatory markers. *iNOS* is expressed at high rates in normal healthy mice's small intestine (ileum) (Matziouridou et al., 2018). As regular *iNOS* expression is high in the ileum, small changes in expression will go largely unnoticed. Consequently, one could argue that *iNOS* is not a very sensitive marker of inflammation in the small intestine. On the other hand, *TNF-α* is a powerful pro-inflammatory cytokine that is well established to be upregulated during inflammation in the small intestine (Bamias et al., 2013; Popa et al., 2007). Like *iNOS*, *TNF-α* was not upregulated in any of the mice. Thus, it seems unlikely that other markers of inflammation would have shown different results to ours.

Gene expression analysis of *ZO-1* revealed significant differences between the groups. Interestingly, the gene was upregulated in the Che7 (HF diet) group compared to the Chow group (low-fat). Furthermore, there was a trend (p-value=0.1328) that *ZO-1* was upregulated in But2 (HF) compared to Chow (low-fat), yet not significant. The results may suggest that HF-mice exhibit improved barrier functions, characterised by an increase in tight junction proteins. These observations are surprising as many studies have shown that a HF diet increases the intestinal barrier's permeability and diminishes the expression of tight junction encoding genes (Lam et al., 2012; Mujawdiya et al., 2020; Murakami et al., 2016; Suzuki & Hara, 2010).

Hamilton et al. (2015) found the paracellular permeability in the ileum to be increased in HF-mice compared to low-fat Chow control mice after 1 week. However, permeability in HF-mice returned to control values at weeks 3 and 6. Additionally, they found the tight junction gene *ZO-1* to be significantly more expressed at week 3 than weeks 1 and 6. The authors argue that the tight junction gene *ZO-1* is upregulated as part of a compensatory mechanism to return permeability to normal levels. The mechanism proposed by Hamilton could potentially explain our findings: the Che7 and But2 mice upregulate the expression of *ZO-1* to compensate for increased paracellular permeability caused by a HF

diet. However, as we did not test the permeability of the barrier, it is impossible to confirm this hypothesis.

Furthermore, we discovered a significant effect of matrix (p-value=0.004) on the expression of the tight junction gene *ZO-1*. To our knowledge, no other studies have looked at the effect of dairy matrices on body weight development and barrier functions in humans or animals. However, one study demonstrated that peptides derived from cheese (Mozzarella) increased expression of ZO-1 in mouse small intestine (Tenore et al., 2019) and another study showed that lactic acid bacteria used in cheese production also increased ZO-1 (Cordeiro et al., 2021). To what extent these factors contributed in our study was not investigated, and we can only speculate whether these nutrients or ingredients were responsible for the observed matrix effect on ZO-1 expression.

In summary, no differences in inflammatory status were observed as an effect of Ca. The tight junction gene ZO-1 was upregulated in But2 and Che7 compared to the Chow, which may have been a regulatory mechanism to adjust for increased intestinal barrier permeability due to a HF diet. However, further research is needed to elucidate these results.

5.4 The Minispec LF50 from Bruker accurately measures body fat in live mice

We performed a small experiment to evaluate the accuracy of the body fat readings from Bruker's Minispec LF50. The NMR instrument recorded the fat mass of 10 mice before we sacrificed the animals and dissected the large fat depots (gonadal/epidydimal and visceral fat). A correlation analysis revealed the NMR measurements and weight of the fat depots to be highly correlated (r=0.9677 and P-value<0.0001) (shown as a linear regression plot in Figure 4.8.A).

Halldorsdottir et al. performed a worthwhile experiment comparing fat mass measurements of the Minispec LF50 instrument against fat extracted through chemical carcass analysis (Halldorsdottir et al., 2009). Chemical carcass analysis will give a value close to the actual fat mass of the carcass (Dobush et al., 1985), making it an ideal comparison. They found the NMR fat mass measurements and fat extracted from the carcass to be highly correlated (r^2=0.99, P-value<0.001).

Furthermore, Halldorsdottir evaluated the within-day variation of NMR measurements by scanning each mouse four times in one day (n=30) (Halldorsdottir et al., 2009). They found the relative standard deviation of the fat mass readings to be 2.8%. These results agree with the findings of Jiang et al. who scanned lean and obese mice ten times in a single day with an NMR instrument and observed the relative standard deviation of fat mass to be 2.04% and 0.69%, respectively (Jiang et al., 2020).

Indeed, our results and that of others (Halldorsdottir et al., 2009; Jiang et al., 2020) indicate that the TD-NMR technology is proficient at predicting the fat mass in live mice. However, the fat readings from the

main experiment are characterised by unpredictability during the two last weeks of the experiment. As the software crashed during the last week of the experiment, technical support from Bruker was contacted. A problem with the syncing between the electronics and software was identified, and subsequently fixed by a reboot of the system. Most likely, the variations observed during the latter part of the experiment was caused by the syncing problem.

5.5 Methodological considerations

There are many advantages of using mice as research animals. They are small and easily maintained, cost-effective, easy to breed and genetically modify. In addition, they have a short lifespan (1 human year is equivalent to 30 mice years), which means that long term developments can be researched in a reasonable time frame. Mice are valuable within nutritional research as their food intake can be fully controlled. However, it is vital to show caution when translating effects on mice to that of humans. While mice and humans have genomes with 85% identical protein-coding regions, their lineages are thought to have diverged 85 million years ago (Perlman, 2016). Hence, mice are different from humans in many ways, most notably in their size. Some differences are also observed in the GI tract; the length of the small intestine compared to the large intestine is much greater in mice than in humans. Despite their limitations, mice models have been essential to many scientific fields' progress and will continue to do so until better alternatives are discovered.

A weakness of our study design was the lack of a low-Ca cheese group. The Ca of the Norvegia Vellagret made the natural Ca content of the feed 7 g per kg. Thus, making a cheese feed with less than 7 g Ca per kg would not have been possible. Including a low-Ca cheese group would have made it possible to run a two-way ANOVA that included the low-Ca, mid-Ca and high-Ca groups. However, only the mid-and high-Ca groups were included due to the nature of a two-way ANOVA. This was unfortunate, as differences in, e.g., apparent digestibility, were more severe between the low-Ca and mid-Ca groups than between the mid-Ca and high-Ca groups (as seen in Table 4.1.).

6 CONCLUSION

Our results show that Ca impacts SFA digestibility in mice receiving HF diets in a dose-dependent manner. High levels of Ca led to increasing amounts of SFAs in the faeces. Long chain SFAs were most affected. However, the effect was minor compared to what other studies have found, which may be explained by a sub-optimal system for CS precipitation.

Furthermore, we found that the low-Ca butter group gained significantly more weight than the high-Ca butter group over five weeks. The difference in weight gain is probably not explained by faecal fat excretion but rather an increased metabolic activity in the high-Ca mice. While no matrix effect was observed on 16:0 and 18:0 digestibility, there was a trend that matrix affected the weight development of the mice.

Ca did not affect the expression of the inflammatory markers *TNF-α*, *iNOS* and *NOX2*. However, the tight junction gene *ZO-1* was upregulated in the low-Ca/HF butter diet and mid-Ca/HF cheese diet compared to the low-fat Chow control diet. This may have been a regulatory mechanism to adjust for increased intestinal barrier permeability caused by HF feeding. In addition, the matrix was found to significantly influence the expression of the tight junction gene *ZO-1*, with a higher expression being observed in the cheese-based diets.

Finally, the NMR instrument emerged as a reliable and good predictor of body fat mass in mice. NMR fat measurements of the mice were highly correlated with the weight of large fat depots dissected out of the same mice.

7 FUTURE PERSPECTIVES

To further examine the relationship between calcium and weight development, it would have been interesting to evaluate insulin sensitivity in the mice. We measured fasting glucose in the mice before they were sacrificed, with the intent to evaluate insulin sensitivity through the Homeostatic Model Assessment for Insulin Resistance (HOMA-IR). However, we choose not to perform the insulin ELISA assay due to time limitations caused by multiple lockdowns due to Covid-19.

We discovered significant differences in the expression of a tight junction gene and argued that this could be a compensatory mechanism to adjust for increased permeability of the intestinal barrier. It would have been interesting to test this argument by evaluating the barrier's permeability by, for instance, a FITC-dextran assay. Furthermore, it would be interesting to test permeability at several time points during the experiment to understand the dynamics and adjustability of the barrier better.

At the end of the 5-week trial, the HF mice showcased a slightly overweight phenotype, yet did not become obese. Still, we observed significant differences in total weight gain between the groups. It would have been interesting to see if an extended experiment would have exaggerated the effect of Ca as the animals reach an obese phenotype. Furthermore, a lengthier experiment would most likely have induced inflammation in the small intestine of the HF mice, which may be attenuated by increasing levels of Ca.

Since we observed that increased weight was negatively associated with calcium in the feed combined with the notion that decreased fat uptake cannot account for these differences, it would be desirable to assess the metabolic activity of mice during the feeding trial. It is not unlikely that mice fed high calcium expend more energy in e.g., producing more bile. Such an experiment is challenging as it requires the use of specialized metabolic cages which can measure accurately metabolic rates in individual mice during a specified time period.

References

Alexander, D. D., Bylsma, L. C., Vargas, A. J., Cohen, S. S., Doucette, A., Mohamed, M., Irvin, S. R., Miller, P. E., Watson, H. & Fryzek, J. P. (2016). Dairy consumption and CVD: a systematic review and meta-analysis. *Br J Nutr*, 115 (4): 737-50. doi: 10.1017/s0007114515005000.

Alomaim, H., Griffin, P., Swist, E., Plouffe, L. J., Vandeloo, M., Demonty, I., Kumar, A. & Bertinato, J. (2019). Dietary calcium affects body composition and lipid metabolism in rats. *PLoS One*, 14 (1): e0210760. doi: 10.1371/journal.pone.0210760.

Ayala-Bribiesca, E., Turgeon, S. L., Pilon, G., Marette, A. & Britten, M. (2018). Postprandial lipemia and fecal fat excretion in rats is affected by the calcium content and type of milk fat present in Cheddar-type cheeses. *Food Res Int*, 107: 589-595. doi: 10.1016/j.foodres.2018.02.058.

Azam, S., Jakaria, M., Kim, I.-S., Kim, J., Haque, M. E. & Choi, D.-K. (2019). Regulation of Toll-Like Receptor (TLR) Signaling Pathway by Polyphenols in the Treatment of Age-Linked Neurodegenerative Diseases: Focus on TLR4 Signaling. *Frontiers in immunology*, 10: 1000-1000. doi: 10.3389/fimmu.2019.01000.

Ballweg, S., Sezgin, E., Doktorova, M., Covino, R., Reinhard, J., Wunnicke, D., Hänelt, I., Levental, I., Hummer, G. & Ernst, R. (2020). Regulation of lipid saturation without sensing membrane fluidity. *Nature Communications*, 11 (1): 756. doi: 10.1038/s41467-020-14528-1.

Bamias, G., Dahman, M. I., Arseneau, K. O., Guanzon, M., Gruska, D., Pizarro, T. T. & Cominelli, F. (2013). Intestinal-Specific TNFα Overexpression Induces Crohn's-Like Ileitis in Mice. *PLOS ONE*, 8 (8): e72594. doi: 10.1371/journal.pone.0072594.

Breil, C., Abert Vian, M., Zemb, T., Kunz, W. & Chemat, F. (2017). "Bligh and Dyer" and Folch Methods for Solid-Liquid-Liquid Extraction of Lipids from Microorganisms. Comprehension of Solvatation Mechanisms and towards Substitution with Alternative Solvents. *International journal of molecular sciences*, 18 (4): 708. doi: 10.3390/ijms18040708.

Cani, P. D., Possemiers, S., Van de Wiele, T., Guiot, Y., Everard, A., Rottier, O., Geurts, L., Naslain, D., Neyrinck, A., Lambert, D. M., et al. (2009). Changes in gut microbiota control inflammation in obese mice through a mechanism involving GLP-2-driven improvement of gut permeability. *Gut*, 58 (8): 1091-1103. doi: 10.1136/gut.2008.165886.

Carta, G., Murru, E., Banni, S. & Manca, C. (2017). Palmitic Acid: Physiological Role, Metabolism and Nutritional Implications. *Frontiers in physiology*, 8: 902-902. doi: 10.3389/fphys.2017.00902.

Chei, C.-L., Yamagishi, K., Kitamura, A., Kiyama, M., Sankai, T., Okada, T., Imano, H., Ohira, T., Cui, R., Umesawa, M., et al. (2018). Serum Fatty Acid and Risk of Coronary Artery Disease — Circulatory Risk in Communities Study (CIRCS) —. *Circulation Journal*, 82 (12): 3013-3020. doi: 10.1253/circj.CJ-18-0240.

Chen, L., Deng, H., Cui, H., Fang, J., Zuo, Z., Deng, J., Li, Y., Wang, X. & Zhao, L. (2017). Inflammatory responses and inflammation-associated diseases in organs. *Oncotarget*, 9 (6): 7204-7218. doi: 10.18632/oncotarget.23208.

Chistiakov, D. A., Bobryshev, Y. V., Kozarov, E., Sobenin, I. A. & Orekhov, A. N. (2015). Intestinal mucosal tolerance and impact of gut microbiota to mucosal tolerance. *Frontiers in microbiology*, 5: 781-781. doi: 10.3389/fmicb.2014.00781.

Clemente, G., Mancini, M., Nazzaro, F., Lasorella, G., Rivieccio, A., Palumbo, A. M., Rivellese, A. A., Ferrara, L. & Giacco, R. (2003). Effects of different dairy products on postprandial

lipemia. *Nutrition, Metabolism and Cardiovascular Diseases*, 13 (6): 377-383. doi: https://doi.org/10.1016/S0939-4753(03)80007-8.

Cohen, P. & Spiegelman, B. M. (2016). Cell biology of fat storage. *Molecular Biology of the Cell*, 27 (16): 2523-2527. doi: 10.1091/mbc.e15-10-0749.

Cordeiro, B. F., Alves, J. L., Belo, G. A., Oliveira, E. R., Braga, M. P., da Silva, S. H., Lemos, L., Guimarães, J. T., Silva, R., Rocha, R. S., et al. (2021). Therapeutic Effects of Probiotic Minas Frescal Cheese on the Attenuation of Ulcerative Colitis in a Murine Model. *Front Microbiol*, 12: 623920. doi: 10.3389/fmicb.2021.623920.

Davies, K. M., Heaney, R. P., Recker, R. R., Lappe, J. M., Barger-Lux, M. J., Rafferty, K. & Hinders, S. (2000). Calcium Intake and Body Weight1. *The Journal of Clinical Endocrinology & Metabolism*, 85 (12): 4635-4638. doi: 10.1210/jcem.85.12.7063.

Dayton, S., Hashimoto, S. & Pearce, M. L. (1965). Influence of a diet high in unsaturated fat upon composition of arterial tissue and atheromata in man. *Circulation*, 32 (6): 911-24. doi: 10.1161/01.cir.32.6.911.

de La Serre, C. B., Ellis, C. L., Lee, J., Hartman, A. L., Rutledge, J. C. & Raybould, H. E. (2010). Propensity to high-fat diet-induced obesity in rats is associated with changes in the gut microbiota and gut inflammation. *American journal of physiology. Gastrointestinal and liver physiology*, 299 (2): G440-G448. doi: 10.1152/ajpgi.00098.2010.

de Lorgeril, M., Salen, P., Martin, J. L., Monjaud, I., Delaye, J. & Mamelle, N. (1999). Mediterranean diet, traditional risk factors, and the rate of cardiovascular complications after myocardial infarction: final report of the Lyon Diet Heart Study. *Circulation*, 99 (6): 779-85. doi: 10.1161/01.cir.99.6.779.

de Oliveira Otto, M. C., Mozaffarian, D., Kromhout, D., Bertoni, A. G., Sibley, C. T., Jacobs, D. R., Jr. & Nettleton, J. A. (2012). Dietary intake of saturated fat by food source and incident cardiovascular disease: the Multi-Ethnic Study of Atherosclerosis. *The American Journal of Clinical Nutrition*, 96 (2): 397-404. doi: 10.3945/ajcn.112.037770.

de Wit, N. J. W., Bosch-Vermeulen, H., Oosterink, E., Müller, M. & van der Meer, R. (2011). Supplementary dietary calcium stimulates faecal fat and bile acid excretion, but does not protect against obesity and insulin resistance in C57BL/6J mice. *British Journal of Nutrition*, 105 (7): 1005-1011. doi: 10.1017/S0007114510004654.

Devraj, R., Williams, H. D., Warren, D. B., Mullertz, A., Porter, C. J. H. & Pouton, C. W. (2013). In vitro digestion testing of lipid-based delivery systems: Calcium ions combine with fatty acids liberated from triglyceride rich lipid solutions to form soaps and reduce the solubilization capacity of colloidal digestion products. *International Journal of Pharmaceutics*, 441 (1): 323-333. doi: https://doi.org/10.1016/j.ijpharm.2012.11.024.

Dhall, S., Wijesinghe, D. S., Karim, Z. A., Castro, A., Vemana, H. P., Khasawneh, F. T., Chalfant, C. E. & Martins-Green, M. (2015). Arachidonic acid-derived signaling lipids and functions in impaired healing. *Wound repair and regeneration : official publication of the Wound Healing Society [and] the European Tissue Repair Society*, 23 (5): 644-656. doi: 10.1111/wrr.12337.

Ding, S., Chi, M. M., Scull, B. P., Rigby, R., Schwerbrock, N. M. J., Magness, S., Jobin, C. & Lund, P. K. (2010). High-fat diet: bacteria interactions promote intestinal inflammation which precedes and correlates with obesity and insulin resistance in mouse. *PloS one*, 5 (8): e12191-e12191. doi: 10.1371/journal.pone.0012191.

Dobush, G. R., Ankney, C. D. & Krementz, D. G. (1985). The effect of apparatus, extraction time, and solvent type on lipid extractions of snow geese. *Canadian Journal of Zoology*, 63 (8): 1917-1920. doi: 10.1139/z85-285.

REFERENCES

Drouin-Chartier, J.-P., Tremblay, A. J., Maltais-Giguère, J., Charest, A., Guinot, L., Rioux, L.-E., Labrie, S., Britten, M., Lamarche, B., Turgeon, S. L., et al. (2017). Differential impact of the cheese matrix on the postprandial lipid response: a randomized, crossover, controlled trial. *The American Journal of Clinical Nutrition*, 106 (6): 1358-1365. doi: 10.3945/ajcn.117.165027.

Fattore, E., Bosetti, C., Brighenti, F., Agostoni, C. & Fattore, G. (2014). Palm oil and blood lipid–related markers of cardiovascular disease: a systematic review and meta-analysis of dietary intervention trials. *The American Journal of Clinical Nutrition*, 99 (6): 1331-1350. doi: 10.3945/ajcn.113.081190.

Folch, J., Lees, M. & Sloane Stanley, G. H. (1957). A simple method for the isolation and purification of total lipides from animal tissues. *J Biol Chem*, 226 (1): 497-509.

Fruekilde, M.-B. & Høy, C.-E. (2004). Lymphatic Fat Absorption Varies among Rats Administered Dairy Products Differing in Physiochemical Properties. *The Journal of Nutrition*, 134 (5): 1110-1113. doi: 10.1093/jn/134.5.1110.

Furman, D., Campisi, J., Verdin, E., Carrera-Bastos, P., Targ, S., Franceschi, C., Ferrucci, L., Gilroy, D. W., Fasano, A., Miller, G. W., et al. (2019). Chronic inflammation in the etiology of disease across the life span. *Nature Medicine*, 25 (12): 1822-1832. doi: 10.1038/s41591-019-0675-0.

Govers, M. J., Termont, D. S., Lapré, J. A., Kleibeuker, J. H., Vonk, R. J. & Van der Meer, R. (1996). Calcium in milk products precipitates intestinal fatty acids and secondary bile acids and thus inhibits colonic cytotoxicity in humans. *Cancer Res*, 56 (14): 3270-5.

Graham, D. Y. & Sackman, J. W. (1983). Solubility of calcium soaps of long-chain fatty acids in simulated intestinal environment. *Digestive Diseases and Sciences*, 28 (8): 733-736. doi: 10.1007/BF01312564.

Halldorsdottir, S., Carmody, J., Boozer, C. N., Leduc, C. A. & Leibel, R. L. (2009). Reproducibility and accuracy of body composition assessments in mice by dual energy x-ray absorptiometry and time domain nuclear magnetic resonance. *International journal of body composition research*, 7 (4): 147-154.

Harvey, K. A., Walker, C. L., Pavlina, T. M., Xu, Z., Zaloga, G. P. & Siddiqui, R. A. (2010). Long-chain saturated fatty acids induce pro-inflammatory responses and impact endothelial cell growth. *Clin Nutr*, 29 (4): 492-500. doi: 10.1016/j.clnu.2009.10.008.

Haub, M. D., Simons, T. R., Cook, C. M., Remig, V. M., Al-Tamimi, E. K. & Holcomb, C. A. (2005). Calcium-fortified beverage supplementation on body composition in postmenopausal women. *Nutrition journal*, 4: 21-21. doi: 10.1186/1475-2891-4-21.

Hegyi, P., Maléth, J., Walters, J. R., Hofmann, A. F. & Keely, S. J. (2018). Guts and Gall: Bile Acids in Regulation of Intestinal Epithelial Function in Health and Disease. *Physiological Reviews*, 98 (4): 1983-2023. doi: 10.1152/physrev.00054.2017.

Hjerpsted, J., Leedo, E. & Tholstrup, T. (2011). Cheese intake in large amounts lowers LDL-cholesterol concentrations compared with butter intake of equal fat content. *The American Journal of Clinical Nutrition*, 94 (6): 1479-1484. doi: 10.3945/ajcn.111.022426.

Howard, B. V., Van Horn, L., Hsia, J., Manson, J. E., Stefanick, M. L., Wassertheil-Smoller, S., Kuller, L. H., LaCroix, A. Z., Langer, R. D., Lasser, N. L., et al. (2006). Low-fat dietary pattern and risk of cardiovascular disease: the Women's Health Initiative Randomized Controlled Dietary Modification Trial. *Jama*, 295 (6): 655-66. doi: 10.1001/jama.295.6.655.

Hu, F. B., Stampfer, M. J., Manson, J. E., Rimm, E., Colditz, G. A., Rosner, B. A., Hennekens, C. H. & Willett, W. C. (1997). Dietary fat intake and the risk of coronary heart disease in women. *N Engl J Med*, 337 (21): 1491-9. doi: 10.1056/nejm199711203372102.

Hu, F. B., Stampfer, M. J., Manson, J. E., Ascherio, A., Colditz, G. A., Speizer, F. E., Hennekens, C. H. & Willett, W. C. (1999). Dietary saturated fats and their food sources in relation to the risk of coronary heart disease in women. *The American Journal of Clinical Nutrition*, 70 (6): 1001-1008. doi: 10.1093/ajcn/70.6.1001.

Hu, M., Li, Y., Decker, E. A. & McClements, D. J. (2010). Role of calcium and calcium-binding agents on the lipase digestibility of emulsified lipids using an in vitro digestion model. *Food Hydrocolloids*, 24 (8): 719-725. doi: https://doi.org/10.1016/j.foodhyd.2010.03.010.

Huang, S., Rutkowsky, J. M., Snodgrass, R. G., Ono-Moore, K. D., Schneider, D. A., Newman, J. W., Adams, S. H. & Hwang, D. H. (2012). Saturated fatty acids activate TLR-mediated proinflammatory signaling pathways. *Journal of lipid research*, 53 (9): 2002-2013. doi: 10.1194/jlr.D029546.

Huth, P. J., Fulgoni, V. L., Keast, D. R., Park, K. & Auestad, N. (2013). Major food sources of calories, added sugars, and saturated fat and their contribution to essential nutrient intakes in the U.S. diet: data from the national health and nutrition examination survey (2003–2006). *Nutrition Journal*, 12 (1): 116. doi: 10.1186/1475-2891-12-116.

Iqbal, J. & Hussain, M. M. (2009). Intestinal lipid absorption. *American journal of physiology. Endocrinology and metabolism*, 296 (6): E1183-E1194. doi: 10.1152/ajpendo.90899.2008.

Jiang, X., Zhou, X., Xie, Z., Ni, Z., Lu, R. & Yi, H. (2020). An Adjustable TD-NMR Method for Rapid and Quantitative Analysis of Body Composition in Awake Mice. *Applied Magnetic Resonance*, 51 (3): 241-253. doi: 10.1007/s00723-019-01180-2.

Kamada, N., Seo, S.-U., Chen, G. Y. & Núñez, G. (2013). Role of the gut microbiota in immunity and inflammatory disease. *Nature Reviews Immunology*, 13 (5): 321-335. doi: 10.1038/nri3430.

Kappel, S., Hawkins, P. & Mendl, M. T. (2017). To Group or Not to Group? Good Practice for Housing Male Laboratory Mice. *Animals : an open access journal from MDPI*, 7 (12): 88. doi: 10.3390/ani7120088.

Keys, A., Mienotti, A., Karvonen, M. J., Aravanis, C., Blackburn, H., Buzina, R., Djordjevic, B. S., Dontas, A. S., Fidanza, F., Keys, M. H., et al. (1986). THE DIET AND 15-YEAR DEATH RATE IN THE SEVEN COUNTRIES STUDY. *American Journal of Epidemiology*, 124 (6): 903-915. doi: 10.1093/oxfordjournals.aje.a114480.

Knoop, K. A. & Newberry, R. D. (2018). Goblet cells: multifaceted players in immunity at mucosal surfaces. *Mucosal Immunology*, 11 (6): 1551-1557. doi: 10.1038/s41385-018-0039-y.

Ko, M. K., Saraswathy, S., Parikh, J. G. & Rao, N. A. (2011). The role of TLR4 activation in photoreceptor mitochondrial oxidative stress. *Investigative ophthalmology & visual science*, 52 (8): 5824-5835. doi: 10.1167/iovs.10-6357.

Kulkarni, B. V. & Mattes, R. D. (2014). Lingual lipase activity in the orosensory detection of fat by humans. *American journal of physiology. Regulatory, integrative and comparative physiology*, 306 (12): R879-R885. doi: 10.1152/ajpregu.00352.2013.

Kushi, L. H., Lew, R. A., Stare, F. J., Ellison, C. R., el Lozy, M., Bourke, G., Daly, L., Graham, I., Hickey, N., Mulcahy, R., et al. (1985). Diet and 20-year mortality from coronary heart disease. The Ireland-Boston Diet-Heart Study. *N Engl J Med*, 312 (13): 811-8. doi: 10.1056/nejm198503283121302.

König, J., Wells, J., Cani, P. D., García-Ródenas, C. L., MacDonald, T., Mercenier, A., Whyte, J., Troost, F. & Brummer, R.-J. (2016). Human Intestinal Barrier Function in Health and Disease. *Clinical and translational gastroenterology*, 7 (10): e196-e196. doi: 10.1038/ctg.2016.54.

Lam, Y. Y., Ha, C. W. Y., Campbell, C. R., Mitchell, A. J., Dinudom, A., Oscarsson, J., Cook, D. I., Hunt, N. H., Caterson, I. D., Holmes, A. J., et al. (2012). Increased gut permeability and microbiota change associate with mesenteric fat inflammation and metabolic dysfunction in diet-induced obese mice. *PloS one*, 7 (3): e34233-e34233. doi: 10.1371/journal.pone.0034233.

Larsen, A. T., Sassene, P. & Müllertz, A. (2011). In vitro lipolysis models as a tool for the characterization of oral lipid and surfactant based drug delivery systems. *International Journal of Pharmaceutics*, 417 (1): 245-255. doi: https://doi.org/10.1016/j.ijpharm.2011.03.002.

Lewington, S., Whitlock, G., Clarke, R., Sherliker, P., Emberson, J., Halsey, J., Qizilbash, N., Peto, R. & Collins, R. (2007). Blood cholesterol and vascular mortality by age, sex, and blood pressure: a meta-analysis of individual data from 61 prospective studies with 55,000 vascular deaths. *Lancet*, 370 (9602): 1829-39. doi: 10.1016/s0140-6736(07)61778-4.

Lorenzen, J. K., Nielsen, S., Holst, J. J., Tetens, I., Rehfeld, J. F. & Astrup, A. (2007). Effect of dairy calcium or supplementary calcium intake on postprandial fat metabolism, appetite, and subsequent energy intake. *The American Journal of Clinical Nutrition*, 85 (3): 678-687. doi: 10.1093/ajcn/85.3.678.

Manuelian, C. L., Currò, S., Penasa, M., Cassandro, M. & De Marchi, M. (2017). Characterization of major and trace minerals, fatty acid composition, and cholesterol content of Protected Designation of Origin cheeses. *Journal of Dairy Science*, 100 (5): 3384-3395. doi: https://doi.org/10.3168/jds.2016-12059.

Matziouridou, C., Rocha, S. D. C., Haabeth, O. A., Rudi, K., Carlsen, H. & Kielland, A. (2018). iNOS- and NOX1-dependent ROS production maintains bacterial homeostasis in the ileum of mice. *Mucosal Immunology*, 11 (3): 774-784. doi: 10.1038/mi.2017.106.

Mayerhöfer, T. G., Pahlow, S. & Popp, J. (2020). The Bouguer-Beer-Lambert Law: Shining Light on the Obscure. *Chemphyschem : a European journal of chemical physics and physical chemistry*, 21 (18): 2029-2046. doi: 10.1002/cphc.202000464.

McMahon, D. J., Paulson, B. & Oberg, C. J. (2005). Influence of Calcium, pH, and Moisture on Protein Matrix Structure and Functionality in Direct-Acidified Nonfat Mozzarella Cheese. *Journal of Dairy Science*, 88 (11): 3754-3763. doi: https://doi.org/10.3168/jds.S0022-0302(05)73061-7.

Micha, R., Wallace, S. K. & Mozaffarian, D. (2010). Red and processed meat consumption and risk of incident coronary heart disease, stroke, and diabetes mellitus: a systematic review and meta-analysis. *Circulation*, 121 (21): 2271-2283. doi: 10.1161/CIRCULATIONAHA.109.924977.

Mollica, M. P., Trinchese, G., Cimmino, F., Penna, E., Cavaliere, G., Tudisco, R., Musco, N., Manca, C., Catapano, A., Monda, M., et al. (2021). Milk Fatty Acid Profiles in Different Animal Species: Focus on the Potential Effect of Selected PUFAs on Metabolism and Brain Functions. *Nutrients*, 13 (4). doi: 10.3390/nu13041111.

Moorhead, S. A., Welch, R. W., Barbara, M., Livingstone, E., McCourt, M., Burns, A. A. & Dunne, A. (2006). The effects of the fibre content and physical structure of carrots on satiety and subsequent intakes when eaten as part of a mixed meal. *British Journal of Nutrition*, 96 (3): 587-595. doi: 10.1079/BJN20061790.

Morgan, M. J. & Liu, Z.-g. (2011). Crosstalk of reactive oxygen species and NF-κB signaling. *Cell Research*, 21 (1): 103-115. doi: 10.1038/cr.2010.178.

Mu, H. & Høy, C.-E. (2004). The digestion of dietary triacylglycerols. *Progress in Lipid Research*, 43 (2): 105-133. doi: https://doi.org/10.1016/S0163-7827(03)00050-X.

Muehlhoff, E., Bennett, A. & McMahon, D. (2013). *Milk and dairy products in human nutrition*. Rome: Food and Agriculture Organization of the United Nations (FAO).

Mujawdiya, P. K., Sharma, P., Sharad, S. & Kapur, S. (2020). Reversal of Increase in Intestinal Permeability by Mangifera indica Seed Kernel Extract in High-Fat Diet-Induced Obese Mice. *Pharmaceuticals (Basel, Switzerland)*, 13 (8): 190. doi: 10.3390/ph13080190.

Murakami, Y., Tanabe, S. & Suzuki, T. (2016). High-fat Diet-induced Intestinal Hyperpermeability is Associated with Increased Bile Acids in the Large Intestine of Mice. *Journal of Food Science*, 81 (1): H216-H222. doi: https://doi.org/10.1111/1750-3841.13166.

Murota, K. (2020). Digestion and absorption of dietary glycerophospholipids in the small intestine: Their significance as carrier molecules of choline and n-3 polyunsaturated fatty acids. *Biocatalysis and Agricultural Biotechnology*, 26: 101633. doi: https://doi.org/10.1016/j.bcab.2020.101633.

Månsson, H. L. (2008). Fatty acids in bovine milk fat. *Food & nutrition research*, 52: 10.3402/fnr.v52i0.1821. doi: 10.3402/fnr.v52i0.1821.

Nordic Nutrition Recommendations (2012).

O'Sullivan, T. A., Hafekost, K., Mitrou, F. & Lawrence, D. (2013). Food sources of saturated fat and the association with mortality: a meta-analysis. *American journal of public health*, 103 (9): e31-e42. doi: 10.2105/AJPH.2013.301492.

Papakonstantinou, E., Flatt, W. P., Huth, P. J. & Harris, R. B. (2003). High dietary calcium reduces body fat content, digestibility of fat, and serum vitamin D in rats. *Obes Res*, 11 (3): 387-94. doi: 10.1038/oby.2003.52.

Pedersen, A. M., Bardow, A., Jensen, S. B. & Nauntofte, B. (2002). Saliva and gastrointestinal functions of taste, mastication, swallowing and digestion. *Oral Diseases*, 8 (3): 117-129. doi: https://doi.org/10.1034/j.1601-0825.2002.02851.x.

Pereira, R. F., Valente, A. J., Fernandes, M. & Burrows, H. D. (2012). What drives the precipitation of long-chain calcium carboxylates (soaps) in aqueous solution? *Phys Chem Chem Phys*, 14 (20): 7517-27. doi: 10.1039/c2cp24152h.

Perlman, R. L. (2016). Mouse models of human disease: An evolutionary perspective. *Evolution, medicine, and public health*, 2016 (1): 170-176. doi: 10.1093/emph/eow014.

Pfaffl, M. W. (2001). A new mathematical model for relative quantification in real-time RT-PCR. *Nucleic Acids Res*, 29 (9): e45. doi: 10.1093/nar/29.9.e45.

Popa, C., Netea, M. G., van Riel, P. L. C. M., van der Meer, J. W. M. & Stalenhoef, A. F. H. (2007). The role of TNF-α in chronic inflammatory conditions, intermediary metabolism, and cardiovascular risk. *Journal of Lipid Research*, 48 (4): 751-762. doi: https://doi.org/10.1194/jlr.R600021-JLR200.

Praagman, J., Beulens, J. W. J., Alssema, M., Zock, P. L., Wanders, A. J., Sluijs, I. & van der Schouw, Y. T. (2016). The association between dietary saturated fatty acids and ischemic heart disease depends on the type and source of fatty acid in the European Prospective Investigation into Cancer and Nutrition–Netherlands cohort1,2. *The American Journal of Clinical Nutrition*, 103 (2): 356-365. doi: 10.3945/ajcn.115.122671.

Praagman, J., Vissers, L. E. T., Mulligan, A. A., Laursen, A. S. D., Beulens, J. W. J., van der Schouw, Y. T., Wareham, N. J., Hansen, C. P., Khaw, K.-T., Jakobsen, M. U., et al. (2019). Consumption of individual saturated fatty acids and the risk of myocardial infarction in a UK and a Danish cohort. *International journal of cardiology*, 279: 18-26. doi: 10.1016/j.ijcard.2018.10.064.

Quinlan, P. T., Lockton, S., Irwin, J. & Lucas, A. L. (1995). The relationship between stool hardness and stool composition in breast- and formula-fed infants. *J Pediatr Gastroenterol Nutr*, 20 (1): 81-90. doi: 10.1097/00005176-199501000-00014.

Quinn, Mark T., Ammons, Mary Cloud B. & DeLeo, Frank R. (2006). The expanding role of NADPH oxidases in health and disease: no longer just agents of death and destruction. *Clinical Science*, 111 (1): 1-20. doi: 10.1042/CS20060059.

Reeves, P. G., Nielsen, F. H. & Fahey, G. C., Jr. (1993). AIN-93 purified diets for laboratory rodents: final report of the American Institute of Nutrition ad hoc writing committee on the reformulation of the AIN-76A rodent diet. *J Nutr*, 123 (11): 1939-51. doi: 10.1093/jn/123.11.1939.

Rehman, I., Mahabadi, N., Sanvictores, T. & Rehman, C. I. (2021). Classical Conditioning. In *StatPearls*. Treasure Island (FL): StatPearls Publishing

Copyright © 2021, StatPearls Publishing LLC.

Reid, I. R., Horne, A., Mason, B., Ames, R., Bava, U. & Gamble, G. D. (2005). Effects of Calcium Supplementation on Body Weight and Blood Pressure in Normal Older Women: A Randomized Controlled Trial. *The Journal of Clinical Endocrinology & Metabolism*, 90 (7): 3824-3829. doi: 10.1210/jc.2004-2205.

Řezanka, T., Pádrová, K. & Sigler, K. (2016). Derivatization in Gas Chromatography of Lipids. In Wenk, M. R. (ed.) *Encyclopedia of Lipidomics*, pp. 1-9. Dordrecht: Springer Netherlands.

Rogero, M. M. & Calder, P. C. (2018). Obesity, Inflammation, Toll-Like Receptor 4 and Fatty Acids. *Nutrients*, 10 (4): 432. doi: 10.3390/nu10040432.

Shapses, S. A., Heshka, S. & Heymsfield, S. B. (2004). Effect of calcium supplementation on weight and fat loss in women. *The Journal of clinical endocrinology and metabolism*, 89 (2): 632-637. doi: 10.1210/jc.2002-021136.

Shen, H., Eguchi, K., Kono, N., Fujiu, K., Matsumoto, S., Shibata, M., Oishi-Tanaka, Y., Komuro, I., Arai, H., Nagai, R., et al. (2013). Saturated Fatty Acid Palmitate Aggravates Neointima Formation by Promoting Smooth Muscle Phenotypic Modulation. *Arteriosclerosis, Thrombosis, and Vascular Biology*, 33 (11): 2596-2607. doi: 10.1161/ATVBAHA.113.302099.

Siri-Tarino, P. W., Sun, Q., Hu, F. B. & Krauss, R. M. (2010). Meta-analysis of prospective cohort studies evaluating the association of saturated fat with cardiovascular disease. *The American journal of clinical nutrition*, 91 (3): 535-546. doi: 10.3945/ajcn.2009.27725.

Soerensen, K. V., Thorning, T. K., Astrup, A., Kristensen, M. & Lorenzen, J. K. (2014). Effect of dairy calcium from cheese and milk on fecal fat excretion, blood lipids, and appetite in young men. *The American Journal of Clinical Nutrition*, 99 (5): 984-991. doi: 10.3945/ajcn.113.077735.

Steimle, A., Autenrieth, I. B. & Frick, J.-S. (2016). Structure and function: Lipid A modifications in commensals and pathogens. *International Journal of Medical Microbiology*, 306 (5): 290-301. doi: https://doi.org/10.1016/j.ijmm.2016.03.001.

Suzuki, T. & Hara, H. (2010). Dietary fat and bile juice, but not obesity, are responsible for the increase in small intestinal permeability induced through the suppression of tight junction protein expression in LETO and OLETF rats. *Nutrition & metabolism*, 7: 19-19. doi: 10.1186/1743-7075-7-19.

Tenore, G. C., Pagano, E., Lama, S., Vanacore, D., Di Maro, S., Maisto, M., Capasso, R., Merlino, F., Borrelli, F., Stiuso, P., et al. (2019). Intestinal Anti-Inflammatory Effect of a Peptide Derived from Gastrointestinal Digestion of Buffalo (Bubalus bubalis) Mozzarella Cheese. *Nutrients*, 11 (3). doi: 10.3390/nu11030610.

Terpstra, A. H. M. (2001). Differences between Humans and Mice in Efficacy of the Body Fat Lowering Effect of Conjugated Linoleic Acid: Role of Metabolic Rate. *The Journal of Nutrition*, 131 (7): 2067-2068. doi: 10.1093/jn/131.7.2067.

Tholstrup, T., Høy, C. E., Andersen, L. N., Christensen, R. D. & Sandström, B. (2004). Does fat in milk, butter and cheese affect blood lipids and cholesterol differently? *J Am Coll Nutr*, 23 (2): 169-76. doi: 10.1080/07315724.2004.10719358.

Tichopad, A., Dilger, M., Schwarz, G. & Pfaffl, M. W. (2003). Standardized determination of real-time PCR efficiency from a single reaction set-up. *Nucleic Acids Res*, 31 (20): e122. doi: 10.1093/nar/gng122.

Tomasik, P. J., Wędrychowicz, A., Rogatko, I., Zając, A., Fyderek, K. & Sztefko, K. (2013). Gastric lipase secretion in children with gastritis. *Nutrients*, 5 (8): 2924-2932. doi: 10.3390/nu5082924.

Torcello-Gómez, A., Boudard, C. & Mackie, A. R. (2018). Calcium Alters the Interfacial Organization of Hydrolyzed Lipids during Intestinal Digestion. *Langmuir*, 34 (25): 7536-7544. doi: 10.1021/acs.langmuir.8b00841.

Totland, T. H., Melnæs, B. K., Lundberg-Hallén, N., Helland-Kigen, K. M., Lund-Blix, N. A., Myhre, J. B., Wetting Johansen, A. M., Bjørge Løken, E. & Andersen, L. F. (2012). *Norkost 3* En landsomfattende kostholdsundersøkelse blant menn og kvinner i Norge i alderen 18-70 år, 2010-11.

Tunick, M. H. (1987). Calcium in dairy products. *J Dairy Sci*, 70 (11): 2429-38. doi: 10.3168/jds.S0022-0302(87)80305-3.

van Meer, G., Voelker, D. R. & Feigenson, G. W. (2008). Membrane lipids: where they are and how they behave. *Nature Reviews Molecular Cell Biology*, 9 (2): 112-124. doi: 10.1038/nrm2330.

Vancamelbeke, M. & Vermeire, S. (2017). The intestinal barrier: a fundamental role in health and disease. *Expert review of gastroenterology & hepatology*, 11 (9): 821-834. doi: 10.1080/17474124.2017.1343143.

Varga, T., Czimmerer, Z. & Nagy, L. (2011). PPARs are a unique set of fatty acid regulated transcription factors controlling both lipid metabolism and inflammation. *Biochimica et biophysica acta*, 1812 (8): 1007-1022. doi: 10.1016/j.bbadis.2011.02.014.

Wang, Liu, M., Portincasa, P. & Wang, D. Q. H. (2013). New insights into the molecular mechanism of intestinal fatty acid absorption. *European journal of clinical investigation*, 43 (11): 1203-1223. doi: 10.1111/eci.12161.

Wang, N., Wang, H., Yao, H., Wei, Q., Mao, X.-M., Jiang, T., Xiang, J. & Dila, N. (2013). Expression and activity of the TLR4/NF-κB signaling pathway in mouse intestine following administration of a short-term high-fat diet. *Experimental and therapeutic medicine*, 6 (3): 635-640. doi: 10.3892/etm.2013.1214.

Yilmaz, A., Onen, H. I., Alp, E. & menevse, s. (2012). Real-Time PCR for Gene Expression Analysis. In, pp. 229-254.

Zangenberg, N. H., Müllertz, A., Kristensen, H. G. & Hovgaard, L. (2001). A dynamic in vitro lipolysis model: I. Controlling the rate of lipolysis by continuous addition of calcium. *European Journal of Pharmaceutical Sciences*, 14 (2): 115-122. doi: https://doi.org/10.1016/S0928-0987(01)00169-5.

Zhang, J., Li, Q., Wu, Y., Wang, D., Xu, L., Zhang, Y., Wang, S., Wang, T., Liu, F., Zaky, M. Y., et al. (2019). Cholesterol content in cell membrane maintains surface levels of ErbB2 and confers a therapeutic vulnerability in ErbB2-positive breast cancer. *Cell communication and signaling : CCS*, 17 (1): 15-15. doi: 10.1186/s12964-019-0328-4.

Zong, G., Li, Y., Wanders, A. J., Alssema, M., Zock, P. L., Willett, W. C., Hu, F. B. & Sun, Q. (2016). Intake of individual saturated fatty acids and risk of coronary heart disease in US men and women: two prospective longitudinal cohort studies. *BMJ (Clinical research ed.)*, 355: i5796-i5796. doi: 10.1136/bmj.i5796.

APPENDIXES

Appendix A - Materials

Table A.1: Overview of the materials and chemicals used in the experiment.

Product name	**Supplier**
Chloroform	VWR Chemicals
Methanol	VWR Chemicals
Hydrochloric acid	Sigma-Aldrich
Acetic acid	Honeywell
Diethyl ether	VWR Chemicals
n-Heptane	VWR Chemicals
Eriochrome Black T	Sigma-Aldrich
Sulfuric acid	Supelco
Ethylenediaminetetraacetic acid (EDTA)	Sigma-Aldrich
Iso-Propanol	VWR Chemicals
Metallic sodium (s)	Merck
Borontrifluoride	Sigma-Aldrich
Phosphate-buffered saline (PBS)	Biowest
RNA*later*	Thermo Fischer
Helium	AGA
Fentadon vet	Dechra Veterinary Products AS
Rompun vet	Bayer Animal Health
Zoletil Forte	Virbac

Appendix B - Instruments

Table B.1: Overview of the instruments used in the experiment

Instrument	Supplier
GX-274 ASPEC system	Gilson Inc.
TRACE™ 1310	Thermo Fisher Scientific
Rtx®-2330 capillary column	Restek
ISQ™ QD GC-MS	Thermo Fisher Scientific
Minispec LF50 7.5 Hz	Bruker
Agilent 2100 Bioanalyzer	Agilent Technologies
LightCycler 480 Instrument II	Roche Applied Science
NanoDrop 2000	NanoDrop Technologies

Appendix C – Softwares

Table C.1:. Overview of softwares used in the experiment

Software
Chromeleon v7.2.9
LinRegPCR
Graphpad 9.2.0
2100 Expert Software
LightCycler® 480 Software
Nanodrop 2000/2000c Operating Software

Appendix D – Kits

Table D.1: Overview of the kits used in the experiments.

Software	Supplier
Agilent RNA 6000 Nano Kit	Agilent Techologies
iScript cDNA Synthesis Kit	Bio-Rad Laboratories
NucleoSpin RNA/Protein Purification Kit	Machery Nagel
5x HOT FIREPol EvaGreen qPCR Supermix	Solis BioDyne

Appendix E – Primer sequences

Table E.1: Overview of primers used in the gene expression analysis

Gene	Primer	Sequence (5'->3')	Product length (bp)	Annealing temperatur during RT-PCR
GAPDH	Forward Reverse	CTTCAACAGCAACTCCCACTCTT GCCGTATTCATTGTCATACCAGG	103	60
iNOS	Forward Reverse	GACATTACGACCCCTCCCAC ACTCTGAGGGCTGACACAAG	57	62
NOX2	Forward Reverse	GGGAACTGGGCTGTGAATGA CAGTGCTGACCCAAGGAGTT	147	61
ZO-1	Forward Reverse	GAGAAAGGTGAAACTCTGCTG ACGAGGAGTCGGATGATTTTAGA	148	59
TNF-α	Forward Reverse	CTGTCTACTGAACTTCGGGGTGAT GGTCTGGGCCATAGAACTGATG	88	61

Norges miljø- og biovitenskapelige universitet
Noregs miljø- og biovitskapelege universitet
Norwegian University of Life Sciences

Postboks 5003
NO-1432 Ås
Norway